UNCLASSIFIED

AD NUMBER

AD-359 727

CLASSIFICATION CHANGES

TO **UNCLASSIFIED**

FROM **CONFIDENTIAL**

19990209 195

AUTHORITY

OCA per doc mrkngs and AFATL ltr; 1 Nov 77

THIS PAGE IS UNCLASSIFIED

UNCLASSIFIED

AD NUMBER

AD-359 727

NEW LIMITATION CHANGE

TO **DISTRIBUTION STATEMENT - A**
Approved for public release;
distribution is unlimited.

LIMITATION CODE: 1

FROM **No Prior DoD Distr Scty Cntrl St'mt Assgn'd**

AUTHORITY

AFATL ltr; 1 Nov 77

THIS PAGE IS UNCLASSIFIED

GENERAL DECLASSIFICATION 0 SCHEDULE

IN ACCORDANCE WITH
DOD 5200.1-R & EXECUTIVE ORDER 11652

THIS DOCUMENT IS:

CLASSIFIED BY_____

Subject to General Declassification Schedule of
Executive Order 11652-Automatically Downgraded at
2 Years Intervals- DECLASSIFIED ON DECEMBER 31, 1973 19

BY

Defense Documentation Center
Defense Supply Agency
Cameron Station
Alexandria, Virginia 22314

AD 359727

DEFENSE DOCUMENTATION CENTER

FOR

SCIENTIFIC AND TECHNICAL INFORMATION

CAMERON STATION, ALEXANDRIA, VIRGINIA

REPRODUCTION QUALITY NOTICE

This document is the best quality available. The copy furnished to DTIC contained pages that may have the following quality problems:

- Pages smaller or larger than normal.
- Pages with background color or light colored printing.
- Pages with small type or poor printing; and or
- Pages with continuous tone material or color photographs.

Due to various output media available these conditions may or may not cause poor legibility in the microfiche or hardcopy output you receive.

☐ If this block is checked, the copy furnished to DTIC contained pages with color printing, that when reproduced in Black and White, may change detail of the original copy.

NOTICE: When government or other drawings, specifications or other data are used for any purpose other than in connection with a definitely related government procurement operation, the U. S. Government thereby incurs no responsibility, nor any obligation whatsoever; and the fact that the Government may have formulated, furnished, or in any way supplied the said drawings, specifications, or other data is not to be regarded by implication or otherwise as in any manner licensing the holder or any other person or corporation, or conveying any rights or permission to manufacture, use or sell any patented invention that may in any way be related thereto.

NOTICE:

THIS DOCUMENT CONTAINS INFORMATION AFFECTING THE NATIONAL DEFENSE OF THE UNITED STATES WITHIN THE MEANING OF THE ESPIONAGE LAWS, TITLE 18, U.S.C., SECTIONS 793 and 794. THE TRANSMISSION OR THE REVELATION OF ITS CONTENTS IN ANY MANNER TO AN UNAUTHORIZED PERSON IS PROHIBITED BY LAW.

NOTICE: When government or other drawings, specifications or other data are used for any purpose other than in connection with a definitely related government procurement operation, the U. S. Government thereby incurs no responsibility, nor any obligation whatsoever; and the fact that the Government may have formulated, furnished, or in any way supplied the said drawings, specifications, or other data is not to be regarded by implication or otherwise as in any manner licensing the holder or any other person or corporation, or conveying any rights or permission to manufacture, use or sell any patented invention that may in any way be related thereto.

NOTICE:

THIS DOCUMENT CONTAINS INFORMATION AFFECTING THE NATIONAL DEFENSE OF THE UNITED STATES WITHIN THE MEANING OF THE ESPIONAGE LAWS, TITLE 18, U.S.C., SECTIONS 793 and 794. THE TRANSMISSION OR THE REVELATION OF ITS CONTENTS IN ANY MANNER TO AN UNAUTHORIZED PERSON IS PROHIBITED BY LAW.

359727
CATALOGED BY: DDC
AS AD No.
3 3 1 7 1

AFL-TR-65-12 Copy 4 of 42 Copies

(U) PERSONNEL MARKING AND DETECTION
(Laser Technique)

April 1965

This material contains information affecting the national defense of the United States within the meaning of the Espionage Laws (Title 18, U.S.C., sections 793 and 794), the transmission or revelation of which in any manner to an unauthorized person is prohibited by law.

Directorate of Armament Development
Det 4, Research and Technology Division
Air Force Systems Command
Eglin Air Force Base, Florida

DDC CONTROL NO. 51819

GROUP-4
Downgraded at 3 year intervals;
Declassified after 12 years.

Qualified users may obtain copies of this report from the Defense Documentation Center.

Foreign announcement and dissemination by the Defense Documentation Center is not authorized.

Do not return this copy. When not needed, destroy in accordance with pertinent security regulations.

(U) PERSONNEL MARKING AND DETECTION
(Laser Technique)

April 1965

This material contains information affecting the national defense of the United States within the meaning of the Espionage Laws (Title 18, U.S.C., sections 793 and 794), the transmission or revelation of which in any manner to an unauthorized person is prohibited by law.

GROUP-4
Downgraded at 3 year intervals;
Declassified after 12 years.

(This page is Unclassified)

FOREWORD

The work presented in this report was performed by Isomet Corporation, Palisades Park, New Jersey, under Air Force Contract Number AF08(635)-3734, Personnel Marking and Detection (Laser Technique).

Lt J. R. Clary, Detachment 4, HTD, Bio-Chemical Division, Eglin Air Force Base, Florida, served as Project Officer.

The authors and contributing personnel of Isomet Corporation who cooperated in the study program and the preparation of this report were Mr. Gerald Jankowitz, Project Director, and Dr. Warren Ruderman, President and Senior Engineer, Project 698U.

Publication of this technical documentary report does not constitute Air Force approval of its content. Distribution in this form is intended solely as a means of achieving prompt and efficient dissemination of information. Emphasis has been given to timeliness rather than formality.

[redacted] TABLE OF CONTENTS

		PAGE
1.	Abstract	1
2.	Introduction	2
3.	System Analysis	5
4.	Experimental Program	16
5.	Summary and Conclusions	37
6.	Recommendations	40

[redacted]

[redacted]

FIGURES

NO.	TITLE	SECTION
1	System Geometry	2.2.3
2	Basic Photometer	3.1.2
3	Transmission of the Atmosphere	3.4.2
4	Energy Band Model	3.4.3.4
5	Experimental Set-Up for Energy Measurements	4.1.1
6	Calorimeter for Laser Power Output Measurement	4.1.1
7	Output vs. Input-Helical Flash Tube at Room Temperature	4.1.4
8	Linear Cavity (Mark I)	4.1.5
9	Output vs. Input - Linear Flash Tube at Room Temperature	4.1.5
10	Improved Linear Cavity	4.1.8
11	Ray Tracing for Cylindrical Cavity With Close Spacing	4.1.8
12	Ray Tracing for Cylindrical Cavity with Large Spacing	4.1.8
13	Four Level Laser	4.2.1
14	Laser Timing Requirements	4.2.1
15	Experimental Q-Switched Laser Illuminating System	4.2.3.1
16	Mechanical Q-Switch Assembly (Diagram)	4.2.4.1
17	Mechanical Q-Switching Assembly (Photo)	4.2.4.1
18	Ruby Q-Switched Output	4.2.4.2
19	Pulse Shape of $CaWO_4$ (Nd^{3+}) For Q-Switched and Normal Laser	4.2.4.3
20	Lamp Emission Spectra and Neodymium Absorption Spectra	4.2.7
21	Photometer Head	4.3
22	Narrow Band Pass U.V. Filter	4.4.2.2
23	I.R. Pass Filter	4.4.2.3
24	Water Filter	4.4.2.4
25	1.06 Reject Photometer Filter	4.4.2.4
26	Fluorescence Spectra of CdS (Ag,V)	4.4.3
27	Fluorescence Spectra of ZnS (Cu,V)	4.4.3
28	Fluorescence Spectra of CdSe (Cu,In)	4.4.3
29	Fluorescence Spectra of CdSe-CdS(Cu,In) and CdSe (Cu,In)	4.4.3
30	$CaWO_4$ (Nd^{3+}) Excitation of a Phosphor	4.4.6
31	System Block Diagram	6.2

[redacted]

[redacted]

[redacted]

TABLES

NO.	TITLE	SECTION
1	Threshold Measurements of $CaWO_4$ (Nd^{3+}) Laser Crystals at Room Temperature in a Helical Cavity (FT 524)	4.1.3
2	Threshold Measurements of Neodymium Glass Laser Crystals at Room Temperature in a Helical Cavity (FT 524)	4.1.3
3	Threshold Measurements of Ruby Laser Crystals at Room Temperature in a Helical Cavity (FT 524)	4.1.3
4	Threshold Measurements of $CaWO_4$ (Nd^{3+}) Laser Crystals at Room Temperature in a Linear Cavity (FX-42). Crystal in Glass Shield	4.1.6
5	Threshold Measurements of Neodymium Glass at Room Temperature in a Linear Cavity (FX-42). Crystal in Glass Shield.	4.1.6
6	Threshold Measurements of Ruby at Room Temperature in a Linear Cavity (FX-42). Crystal in Glass Shield	4.1.6
7	Threshold Measurements of Unshielded Ruby, Neodymium Glass and $CaWO_4$ (Nd^{3+}) Crystals at Room Temperature. FX-42 Flash Tube.	4.1.9
8	Threshold Measurements of Unshielded Ruby and $CaWO_4$ (Nd^{3+}) Crystals at Room Temperature. FX-38A Flash Tube.	4.1.10
9	List of Potentially Useful Phosphors Synthesized (UV Excited)	4.4.1.1
10	List of Potential Useful Phosphors Synthesized (IR Excited)	4.4.1.1
11	System Development Schedule	6

[redacted]

[redacted]

[redacted]

[redacted]

1. ABSTRACT

Calculations and experimental studies have been made of the Isomet system for marki[redacted]ction of individuals. Results of these studies i[redacted]that the system is feasible. Recommendations are presented for the further development of this weapon system.

[redacted]

[redacted]

[redacted]

2. INTRODUCTION

2.1 Air Force Requirements in Marking and Detection

What is required is an advanced concept for airborne delivery and application of marking chemicals that will provide a means for marking enemy personnel so they can be distinguished from friendly individuals. It is also desired to track marked enemy personnel. It is assumed that both friendly and enemy groups may be living in the same area.

The system shall be:

1. Compatible with tactical and support aircraft both present and programmed.

2. Sufficiently versatile to permit delivery of the marking chemical and subsequent identification of the target at high and low altitudes and within the speed range of the delivery vehicle.

3. Applicable at long ranges from high speed aircraft.

4. Capable of utilizing a marking agent having a minimum effective life of ten days and a useable lifetime of thirty days.

5. Suitable for tracking as well as for identification of personnel.

6. Capable of utilizing a marking agent which is not harmful or toxic to the individuals marked.

7. Imperceptible to the individuals marked.

2.2 The Isomet Marking and Detection System

The basic concepts of the Isomet system comprise marking individuals with a phosphor which can be excited by the directed illumination of a laser device contained in an aircraft. The radiation emitted by the laser as well as the return light signal from the phosphor are both in the infrared or ultraviolet region of the spectrum and hence invisible to the naked eye.

[redacted]

2.2.2 Sector-Po[redacted]SPM)

The Isomet concept is a double marking technique. Each individual in a village is covertly marked with a phosphor which is characteristic for the village and indicates his origin. This marking will be referred to as "sector" marking. An individual seen visually from the air can be marked with a chemical agent by a dissemination device or munition from the aircraft. If the individual already has sector marking, the detection equipment in the aircraft will automatically locate him and indicate his position on a read-out device. He then can be marked again with a different phosphor emitting at another wavelength. A sector marked individual would thus receive an additional "point" marking and would therefore be doubly marked. An individual who is not sector marked would receive only a point marking. The SPM system offers the following advantages:

1. People living in countries such as Vietnam normally do not move far from their villages during their usual living routine. It is, therefore, reasonable to expect that a sector marked individual seen a great distance from his village is engaged in an unusual activity and is hence suspect. The characteristic emission of the sector marking agent immediately indicates his origin.

2. A close range covert observation station in each village can be used to ascertain whether individuals from another village, already marked in their village, have entered. Thus the sector marking enables local surveillance of the population for infiltration elements.

3. Sector marking can be applied under more controlled conditions than point marking and can, therefore, be made more adherent and longer lasting.

4. Emission from sector marking is in general more desirable in the part of the spectrum invisible to the naked eye but easily detectable by ultraviolet or infrared detectors. This enables sensitive detection of sector marked individuals from the air by automatic equipment, and does not require visual observation by the pilot.

5. A doubly marked individual does not need to be tracked, but can be at once identified when passing through a check-point,

since his village or origin is known and the point marking indicates that he has been in an area remote from his village.

2.2.1 System Description

The marking agent is a phosphor, preferably of one of the following types: infrared excited and infrared emitting; ultraviolet excited and ultraviolet emitting; or ultraviolet excited and infrared emitting. A phosphor of any of these types would not be visible to the individual marked, nor would the exciting source used for detection be visible.

The exciting source consists of a short-duration high peak power output laser pulse of a wavelength suitable for excitation of the phosphor. As shown in Figure 1, the aircraft at an altitude, R, emits a laser pulse having a radiation pattern of angular width, Ø, in the direction perpendicular to the line of flight and, Θ, in the direction parallel to the line of flight. An emitting source within the field of view is excited by the laser source and re-emits a characteristic radiation. The detection optics, in the aircraft, has the same field of view as the laser source. It collects the signal and transfers it to the detection and correlation electronics. The latter produces a read-out which indicates the location of the individual who can then be point marked.

SECRET

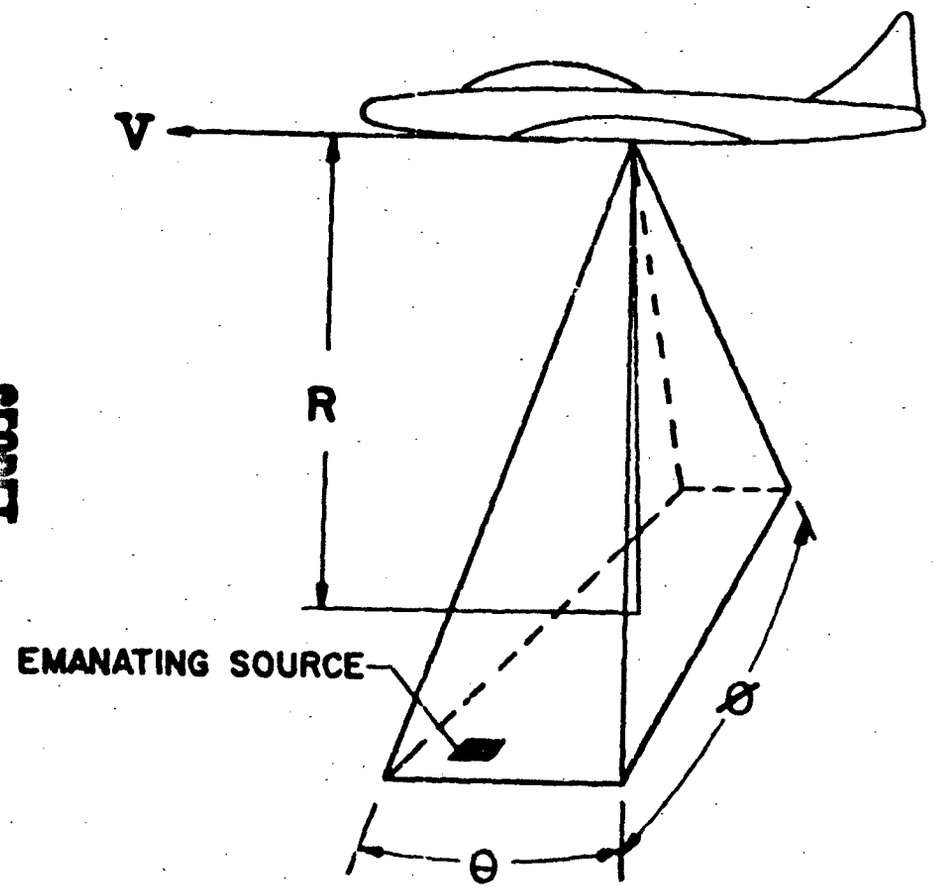

Figure 1. System Geometry

SECRET

3. SYSTEM ANALYSIS

The weapons system consists of three basic units: the transmitter, the phosphor sample and the optical receiver. This analysis is a derivation of the relationships for each subsystem and for the overall system.

The results of the analysis are expressed in terms of the maximum operating range and the maximum aircraft velocity to altitude ratio (V/H) at which the system can be operated.

3.1 General (S/N) Analysis

The receiver will be a photometer capable of responding to the emission spectrum and only the emission spectrum of the tested phosphrs. The photometer time constant, τ, will be determined by the detector circuitry. The field of view of the receiver optics will be determined by the radiation pattern of the transmitter.

3.1.1 Signal Level

The invisible radiation emitted by the phosphor incident on the clear optical aperture of the photometer is the signal power. If the total phosphor area, A_p, in the field of view has a detectable brightness, N_p, then the signal level, S, will be:

$$(1) \quad S = \frac{D_o^2 N_p A_p}{4R^2} \quad \text{(watts)}$$

Where R = Range
and D_o = clear aperture of the photometer.

The phosphor area has been illuminated by the transmitter source which uniformly radiates its output power over a rectangular field of dimension ΘR by ΨR. The surface brightness N_p, after conversion in the phosphor with an efficiency K_1 will be,

$$(2) \quad N_p = \frac{K_1(P.P)}{\Theta \Psi R^2} \quad \text{(watts/cm}^2\text{)}$$

where P.P = excitation energy (watts)
Substituting equation (2) into equation (1) will yield,

$$(3)\quad S = \frac{K_1 (P.P) D_o^2 A_p}{400 R^4} \quad \text{(watts)}$$

Equation 3 gives the signal power detected by the photometer.

3.1.2 Noise Level

It is assumed that the system can be made detector noise limited with present state of the art techniques. Therefore for this analysis detector noise is assumed to be the limiting factor in the photometer. The electrical noise output of the detector can be converted by its responsivity to an equivalent noise input power, commonly called the noise equivalent power, NEP. Since the optical system is for all intensive purposes lossless, the detector NEP will be equal to the noise equivalent power at the photometer entrance aperture.

The NEP of a circular detector is determined by the detector size, the time constant of the detector preamplifier assembly, τ, and a constant for the detector material, the detectivity (D^*). The relationship for NEP is,

$$(4)\quad NEP = \frac{D_d}{2\sqrt{2}\, D^* \sqrt{\tau}} \quad \text{(watts)}$$

The minimum detector diameter, D_d, is determined by the photometer optics, a layout of which is shown in Figure 2.

This analytical photometer consists of an objective lens, a field lens and a detector. The objective lens forms an image in the plane of the field lens of all objects in the field of view. The field lens is designed to image the objective lens onto the detector surface. Since the objective surface is illuminated uniformly, its image will also be uniform. The minimum detector diameter, D_d, is the diameter of the image of the entrance pupil, D_o', and is

$$(5)\quad D_d = D_o' = D_o \frac{f_f}{f_o}$$

where f_f = focal length of field lens
f_o = focal length of objective lens

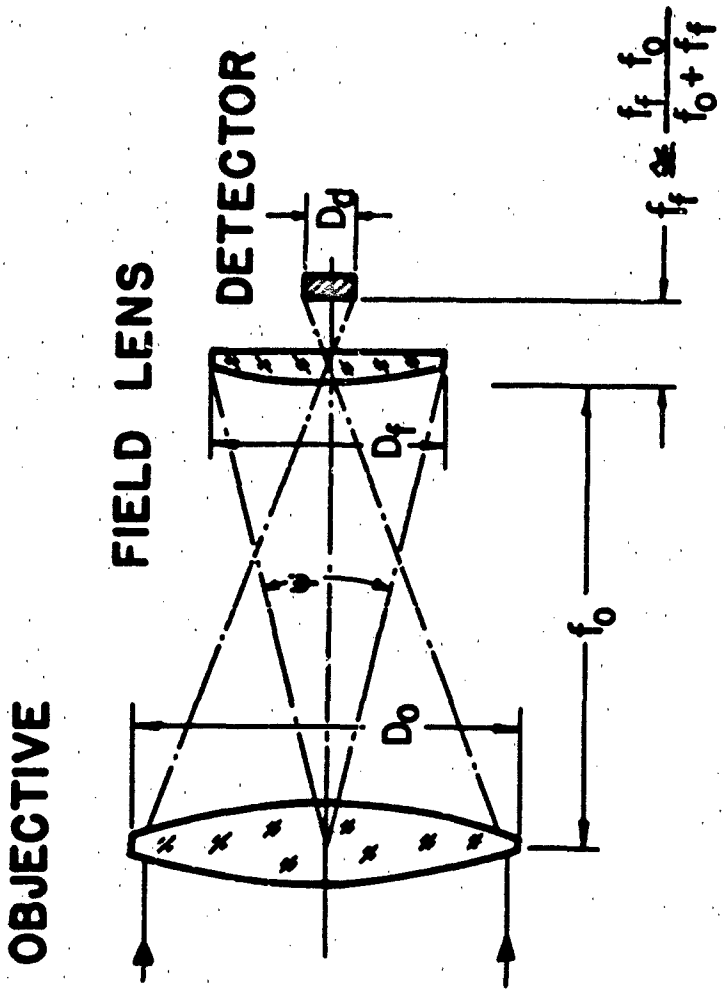

Figure 2. Basic Photometer

If the detector is smaller, there will be a reduction of signal level, since the entire clear aperture is not used.

The maximum angular width of the field of view, ψ, determines the diameter of the field lens D_f,

$$(6) \quad D_f = 2f_o \tan(\psi/2)$$

To simplify equation 6, we may use the fact that the tangent of a small angle can be approximated by the angle (expressed in radians). Since the field of view in a practical situation will be less than a degree wide, the approximation holds and,

$$(7) \quad D_f = f_o \psi$$

Multiplying equation (5) by $D_f/D_f = 1$ yields

$$(8) \quad D_d = D_o \frac{f_f}{D_f} \frac{D_f}{f_o}$$

Using equation (7) and the fact that f_f/D_f is the f-number for the field lens (f#) the minimum detector diameter is found to be,

$$(9) \quad D_d = D_o f\# \psi$$

The noise equivalent power can now be expressed as a function of system parameters by substituting equation (9) into equation (4) with the result,

$$(10) \quad NEP = \frac{D_o f\# \psi}{2\sqrt{2}\, D^*\sqrt{T}} \quad \text{(watts)}$$

where ψ is related to θ and ϕ by the trigometric equation for the diagonal of a rectangle,

$$(11) \quad \psi = [\theta^2 + \phi^2]^{1/2}$$

3.1.3 Spurious Background Signals

Spurious background signals can be generated by background brightness due to solar illumination and by background fluorescence in response to the transmitter illumination. The power

incident on the photometer aperture due to solar radiation, N_{solar}, can be represented by,

$$(12)\quad N_{solar} = \frac{D_o^2 \omega}{4} \int_{\lambda_1}^{\lambda_2} (NEBPD)\, d\lambda$$

where NEBPD is the noise equivalent background power density for the system bandwidth, per unit wavelength and unit area on the ground. The noise equivalent power due to a re-emission with efficiency, K_2, by the background after stimulation by the system radiation source, will be of the same form as that for the signal power.

If the area of the background phosphor is equated to some portion, α, of the entire field of view, equation (3) becomes,

$$(13)\quad N_{back} = \frac{K_2 (P.P) D_o^2 \alpha}{4 R^2} \qquad \text{(watts)}$$

The total effective noise, N_T, in the field is equal to the square root of the sum of the square of all three independent random noise sources and is found by combining equations 10, 12, and 13 such that,

$$(14)\quad N_T = [(NEP)^2 + (N_{solar})^2 + (N_{back})^2]^{1/2}$$

The largest and the only significant noise source anticipated for the system will be the detector. The range and the signal to noise ratio will therefore be determined in this text by using the noise equivalent power from the detector as given in equation (10). The spurious background levels, if observable, will be measured during the feasibility tests.

3.1.4 System Signal to Noise Ratio

The system will detect a signal, S, with a signal to noise ratio, S/N, determined by taking the ratio of equations (3) and (10), and substituting (11), yielding the general relationship,

$$(15)\quad S/N = \frac{K_1 (P.P) D_o A_p D^* [\tau]^{1/2}}{2 f\# R^4 \omega [\sigma^2 + \sigma^2]^{1/2}}$$

Equation (15) is valid as long as the numbers substituted for the system parameters do not generate requirements that are beyond the state-of-the-art.

3.2 V/H Limitations

The weapons system mush check all areas in its search path for marked objects. The forward ground dimension of the beam is the product of the forward system angle, Θ, and the altitude, H. The time between laser pulses, t, is the time between instants of terrain interrogation. If this time inverval is made too long, there will be a section of terrain which cannot be examined. The angle, the altitude, speed and time interval are related by the average number of times, M, that each area in a search swath is checked as,

$$M = \frac{\Theta H}{Vt}$$

When M is greater than one, all areas in a swath are covered at least once. Rearranging terms and letting M = 1, the maximum value of (V/H) may be derived as

$$(16) \quad (V/H)_{max} \leq \frac{\Theta}{t} \qquad (sec^{-1})$$

Note that once the forward radiation angle and the time between pulses are set, the maximum value of V/H is determined independent of other system parameters.

3.3 Range Equation

The prototype shall be operable as long as the signal to noise ratio, S/N, is as high as required for reliable detection. In section 3.1.4, a relationship between S/N and range was established, equation 15. Transposing terms and solving for range gives the maximum range, R_{max},

$$(17) \quad R_{max} = \left[\frac{K_1 (P \cdot P) D_o A_p D^* (\tau)^{1/2}}{\sqrt{2}\, f\#\, (S/N)_{\Theta\phi}\, \psi} \right]^{1/4}$$

Equation 17 shows that the system ceiling, R_{max}, is a function of the fourth root of most system constants and of the eighth root of the overall system time constant. This is most significant in that if any one system parameter is degraded by

as much as a factor of sixteen, the ceiling is reduced by only a factor of two. This type of system is most dependable.

The width of the search swath of terrain, W, will be a function only of the angular beam width, σ, and the range, R, in that,

(18) $W = R\sigma$

The maximum range and the width of the search swath shall be determined by the weapons system parameters.

3.4 Phosphor Analysis

3.4.1 System Requirements

The following characteristics of a phosphor marking agent are desirable:

1. Non-visible excitation and emission.
2. Strong absorption for presently known laser emission wavelengths.
3. Absorption and emission peaks within windows in the atmosphere.
4. Short decay constant (10^{-6} sec.)
5. High radiant efficiency (watts emitted light out/ watts laser radiation in).
6. Stability to water and the atmosphere.
7. Non-toxic to humans.
8. Neutral or non-obtrusive color.
9. Inexpensive.

3.4.2 Choice of Excitation and Emission Spectrum

Since it is desired that the marking and detection system be covert, the excitation source and the phosphor emission should be in the ultraviolet or the infrared. There are, therefore, but three basic phosphor types to be considered: ultraviolet excited and ultraviolet emitting; ultraviolet excited and infrared emitting; and infrared excited and infrared emitting.

The ultraviolet excited phosphors require an ultraviolet laser. The only high intensity ultraviolet laser now available is

UNCLASSIFIED

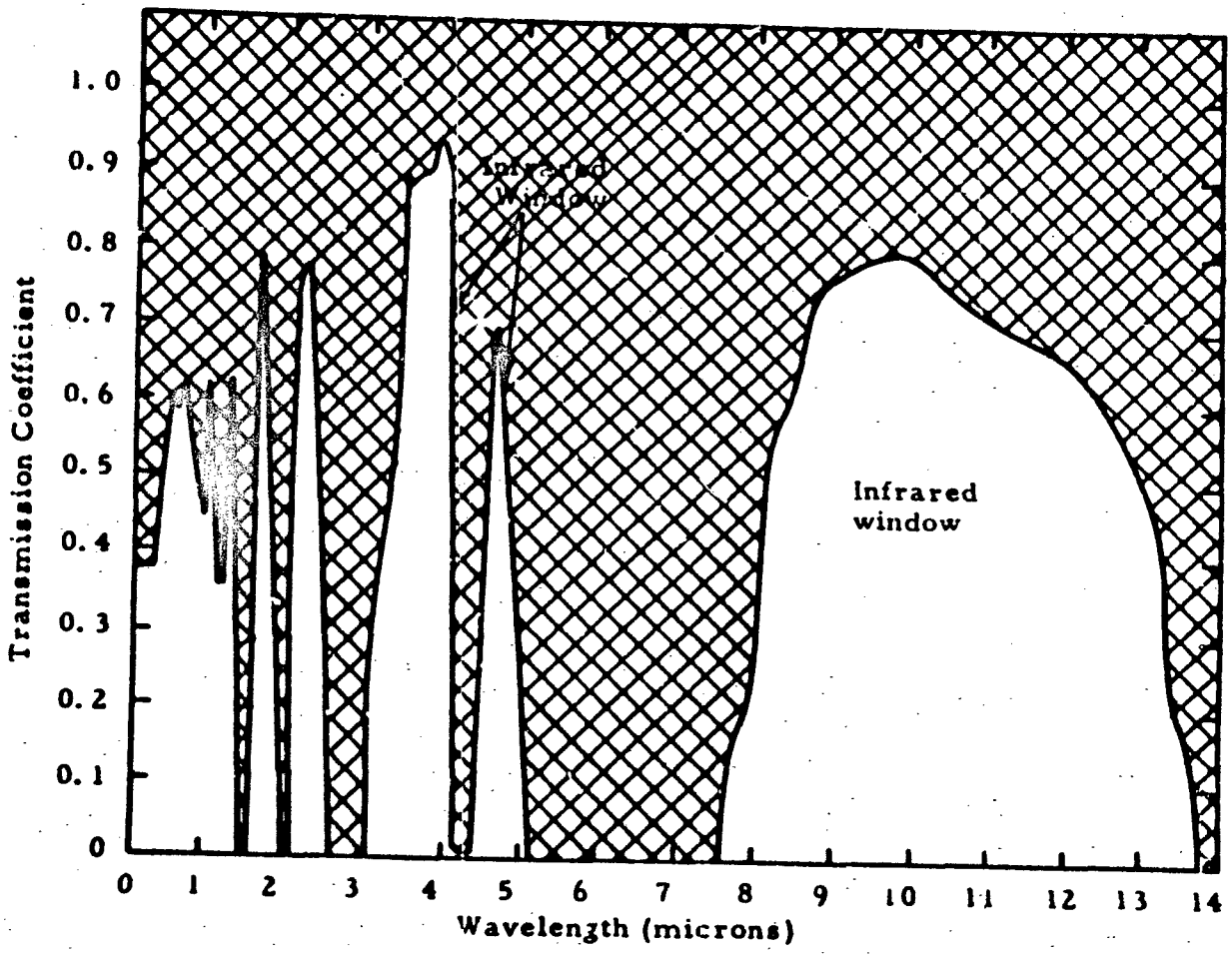

Figure 3. Transmission of the Atmosphere

UNCLASSIFIED

one that depends upon second harmonic generation. A second harmonic of a ruby laser would yield a 3472A source, which is satisfactory for exciting many phosphors. Frequency doubling, however, entails a considerable loss of energy. The highest reported efficiency of conversion of ruby being of the order of 20%.

On the other hand $CaWO_4$ (Nd^{3+}) and neodymium doped glass are more efficient lasers than ruby and if used directly as infrared sources eliminate the energy loss that must be taken if the ruby wavelength is doubled. It is, therefore, highly desirable to use IR-IR phosphors from an energy requirements point of view.

Consider the case of a phosphor that is excited by 3500A radiation, and emits 8000A light with a quantum efficiency of 100%. The 8000A wavelength is chosen because it lies just outside the long wavelength edge of the spectrum visible to the eye. The energy of an emitted 8000A photon is only 44% that of an incident 3500A photon, so that the highest possible radiant efficiency can only be 44%. If the exciting wavelength is 2500A the maximum radiant efficiency drops to 30%. However, if a phosphor is excited by 1.06 micron radiation and emits at 1.2 microns the maximum radiant efficiency is 88%. The IR-IR system has an important potential advantage, therefore, from a radiant efficiency standpoint.

Since the transmitter and receiver are airborne, the excitation and emission wavelengths should fall within windows in the atmosphere. Figure 3 shows the transmission of the atmosphere from the visible to 14 microns in the infrared. The neodymium laser wavelength of 1.06 microns is seen to be satisfactory. Phosphor emission at wavelengths from 1.1 to 1.3 microns, from 1.5 to 1.75 microns, from 2.1 to 2.5 microns and from 3.0 to 4.1 microns will have good atmosphere transmission.

3.4.3 State-of-the-Art of Infrared Emitting Phosphors

3.4.3.1 Introduction

Most of the phosphor research in the past has been directed towards producing visible light, since this spectral region has the greatest practical interest. The literature on infrared emitting phosphors, in general, is very sparse, and negligible on infrared emitting phosphors excited by infrared radiation. A careful search of the literature failed to produce a single reference that treated the case of an infrared emitting phosphor exci-

ted by a narrow bandwidth infrared source, such as would be produced by a neodymium laser.

According to Buillot and Guintine[1] prior to 1950 only two articles appear in the literature on infrared emitting phosphors. One article by Pauli[2] mentions that SrS(Ni) and CaS(Ni) emit in the infrared. The next article appeared in 1946 and mentioned Cu_2O as an infrared emitter. Very little is mentioned in the standard phosphor texts on infrared emitting phosphors. Leverenz[3] seems to ignore infrared emission even when it is evident such as in red emitting phosphors that peak in the infrared. Kroger[4] considers infrared emission but at the time his book was published there was very little in the literature to report.

Less than twelve articles published since 1950 have been found that discuss infrared phosphors. Two review articles by G.F.J. Garlick[5,6], one in 1954 and the other in 1958, treat infrared phosphors. The latest article on infrared phosphors by Bril[7] appeared in 1962.

The infrared phosphors found in the literature were mainly limited to divalent ion crystals. In fact, most of the phosphors reported contained Zn, Cd or Hg combined with S, Se or Te, forming the following series:

ZnS	ZnSe	ZnTe
CdS	CdSe	CdTe
HgS	HgSe	HgTe

1. E. Guillot and P. Guintini, Acad. Sci.-Paris 236.802 (1953)
2. W. E. Pauli, Ann. Phys [4th Series] 34, 750 (1911)
3. H. W. Leverenz, "An Introduction to Luminescence in Solids" (John Wiley & Sons, Inc., New York, 1950).
4. F. A. Kroger "Some Aspects of the Luminescence of Solids" (Elsevier Pub. Co., New York, 1948).
5. G. F. J. Garlick and R. A. Fatehally "Solid State Physics in Electronics and Telecommunications" (Academic Press, London, 1960) Vol. 4, Part 2, p. 741-50.
6. G. F. J. Garlick and M. J. Dumbleton, Proc. Phys. Soc. (London) 67B, 442 (1954).
7. H. P. Kallmann and G. Spruch, "Luminescence of Organic and Inorganic Materials"(John Wiley & Sons, Inc. New York, 1962)p. 479

The only phosphors reported were ZnO, Cu_2O and PbS[5,6,8], also the halogens at temperatures below 180°K and SrS(Ni) and CaS (Ni) which have already been mentioned above.

3.4.3.2 The II-VI Phosphors

The chalcogenides of Zn,Cd and Hg when pure or activated with Cu, Ag or Au give[8,9,10] certain characteristic emission peaks in their luminescent spectra. The series of peaks of each compound is similar to that of the other ones and the peaks move to longer wavelength with increasing weight of the lattice atoms.

ZnS has two well known emission peaks in the visible region - the blue peak at 460 microns and the green peak at 535 microns. The corresponding peaks for a number of other members of the series lie in the infrared (0.8 and 1.0 microns for CdS, 0.92 and 1.2 microns for CdSe). ZnS when prepared in a certain way gives a red emission at 0.67 microns. Browne correlates the observed HgS emission at 2 microns to this red ZnS emission. Browne has also found that ZnS has emission peaks in the infrared region at 1.48 microns and 1.70 microns and that the corresponding CdS peaks are at 1.63 microns and 1.85 microns. He concludes that the blue, green and the infrared emission of ZnS and the corresponding CdS emission arise from one type of fluorescent center; namely a cation vacancy in the crystal lattice that may be empty or may contain a monovalent ion such as Cu, Ag or Au. The emission is characteristic of the lattice anions (S) and not of the activators. He also concludes that the red ZnS emission is due to an anion vacancy.

Browne's studies of ZnS and CdS showed that the anion coactivators (Cl) have a large effect on the efficiency and temperature dependence of the emissions. He divided the phosphors into two classes: (1) those phosphors that can be stimulated by infrared only, and (2) those that need both ultraviolet and infrared stimulation. Some Class 1 phosphors also have their emission enhanced by ultraviolet stimulation. The infrared emission of the Class 2 phosphors that were studied is rather poor at room temperature (estimated to be 10% or less of the quantum yield at low

8. P. F. Browne, J. Electronics 2, 95 (1956).
9. Ibid, 2, 1 (1956)
10. Ibid, 2, 154 (1956)

temperatures). However, the Class 1 phosphors that show no ultraviolet stimulation show much better emission at room temperature (as high as 80% of low temperature emission). These phosphors give very little visible emission and are characterized by being relatively free of coactivator (Cl) and have very little activator. Browne has also shown that heating the ZnS and CdS phosphors in different atmospheres can very strongly affect their emission properties.

3.4.3.3 Vanadium and Cobalt Activators, Indium as a Coactivator

Brill, Avinor and coworkers[1,11-14] have also carried out recent work on CdS and CdSe activated with Cu, Ag, and Au and coactivated with In, a group III-A element. They stimulated infrared emission with ultraviolet and visible light from a high pressure mercury lamp. Coactivation was found to increase the efficiency of emission, and implied that this increase can be obtained in varying degrees with other trivalent ions (III-A elements such as B, Ga, In, Tl, Al).

This group also studies vanadium doped CdS, CdSe, ZnS, and ZnSe, containing Cu, Ag or Au and found that the vanadium quenched the usual emissions but produced an emission peak at about 2.0 microns. These phosphors showed excitation peaks at 0.75 microns and 1.0 microns and are thus infrared stimulable. Garlick[5,6] reported that cobalt doped ZnS shows only infrared emission at 3.3 microns.

3.4.3.4 Luminescence Mechanisms

If we consider the simple energy band model shown in Figure 4 it is seen that the following types of radiative electronic transitions can exist following excitation:

1. Transitions within the emission center.
2. Transitions from the conduction band to empty center.

11. M. Avinor and G. Meijer, J. Chem. Phys. 32,1456 (1960).
12. H. J. Schulz, Phys. Stat. Sol. 3,485 (196?).
13. M. Avinor and G. Meijer, J. Phys. Chem. Solids 12,211 (1960).
14. G. Meijer and M. Avinor, Philips Res. Repts. 15,225 (1960).

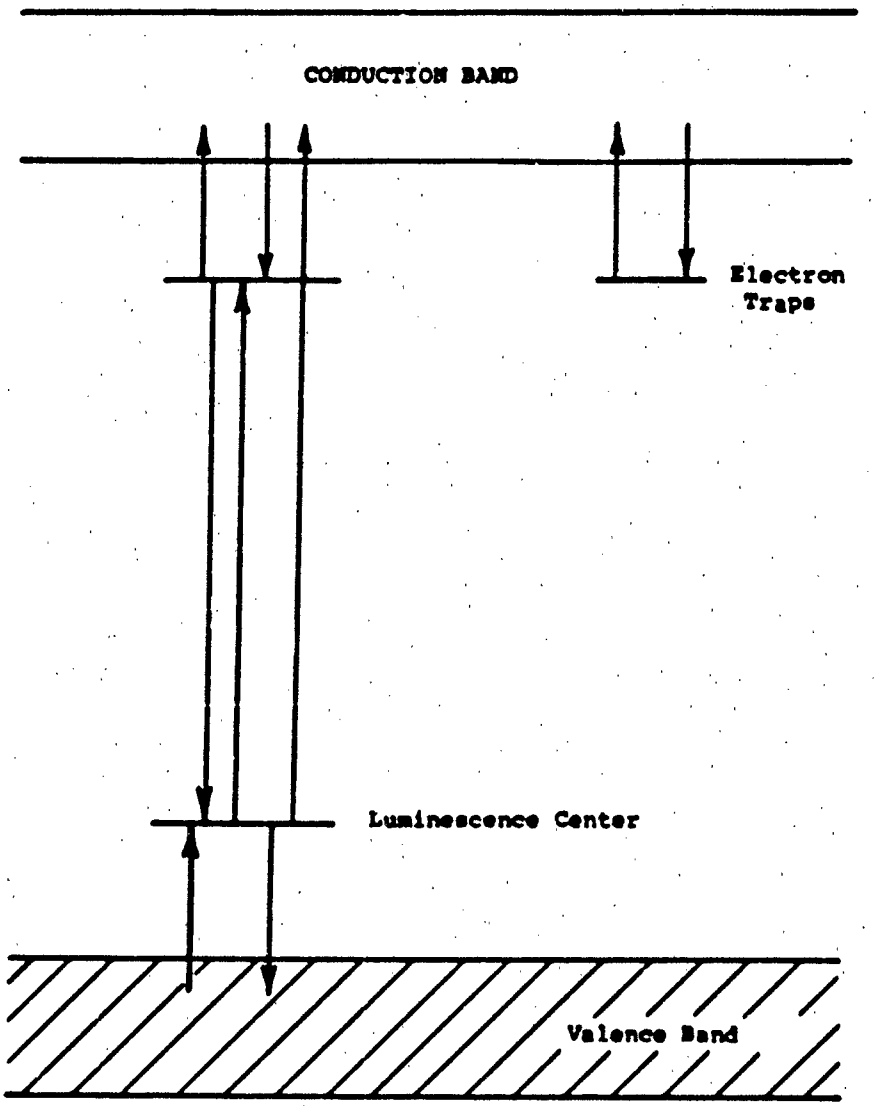

Figure 4 - Energy Band Model

3. Transitions from emission center to empty states or positive hole in the valence band.
4. Transitions into or confined to electron trapping states.

It is quite difficult in any phosphor to assign the proper transition or to define the exact nature of the emitting centers. Let us consider a few of the infrared phosphors that have been studied.

In addition to the well-known visible emission of zinc sulfide and the corresponding near infrared emission of cadmium sulfide, additional bands in the infrared have been found for these phosphors. The excitation spectra for these bands coincide with the quenching spectra of the visible (ZnS) or near visible (CdS) emission of the phosphors. This fact, along with other spectral data, indicate rather conclusively that these infrared bands are associated with transitions between the ground states of the normal emission centers and between these and the valence bands. The emission centers giving the blue and green bands of ZnS, or the corresponding bands in CdS (0.74 and 1.0 microns) are almost certainly due to electrons in or around cation vacancies in the crystal lattice. The levels of the center are due to the perturbed levels of the covalent bands of the surrounding sulfur atom which originally lay in the valence band.

1.4.1.5 Conclusions

A careful search of the technical literature revealed that there is a dearth of information on infrared emitting phosphors. Some recent work has provided a small list of promising materials to be investigated. This list can be used as a guide to the preparation of infrared stimulable and infrared emitting phosphors. The following factors must be considered in the preparation of experimental phosphors: purity of starting materials, flux, temperature of preparation, firing atmosphere, particle size, type and concentration of activator and coactivator. The experimental work must be very careful since small changes in any of the above factors can produce drastic effects on the luminescence.

Some phosphor systems briefly mentioned in the literature but not studied, offer some promise and should be investigated.

4. EXPERIMENTAL PROGRAM

The previous section has shown that if certain requirements are satisfied by the light source (transmitter), the target (phosphor) and the photometer (receiver), the system is a feasible one.

This section describes the experimental effort which has been made to determine the values of the subsystem parameters. The experimental data show that the performance required of the subsystems can be achieved.

4.1 Lasers

The requirements of the laser excitation source are high peak power, high pulse repetition rate, minimum input power and minimum size and weight. It is, therefore, mandatory that the laser system be as efficient as possible; this will reduce input power, minimize cooling, reduce weight and permit high repetition rates. The following sections describe the qualitative and quantitative effort to obtain reliable state of the art data on efficiency. This work has also provided guidelines for significant improvements in efficiency.

4.1.1 Experimental Arrangement for Obtaining Threshold and Energy Data

Threshold energy was measured by sampling the laser beam with a photomultiplier whose output was observed by a Tektronix 555 oscilloscope and photographed. Threshold was taken as that energy level for which a single pulse of laser light was detectable. The photomultiplier was shielded from the lamp light by use of suitable filters. For ruby a No. 32 filter and the necessary neutral density filters were used. For Nd doped glass and $CaWO_4$ a silicon filter was used.

Energy measurements were made by firing the laser beam into a calorimeter. Figure 5 is a photograph of the experimental set up. This calorimeter consists of two graphite cups each coated with finely divided carbon. Thermistor beads are located on the outside of the cup to measure the temperature rise due to absorption of the laser beam entering one cup; the other cup serves as dummy in the standard thermistor bridge circuit and cancels out fluctuations due to ambient temperature. The output is fed into a d.c. amplifier and a recorder. The cups are cali-

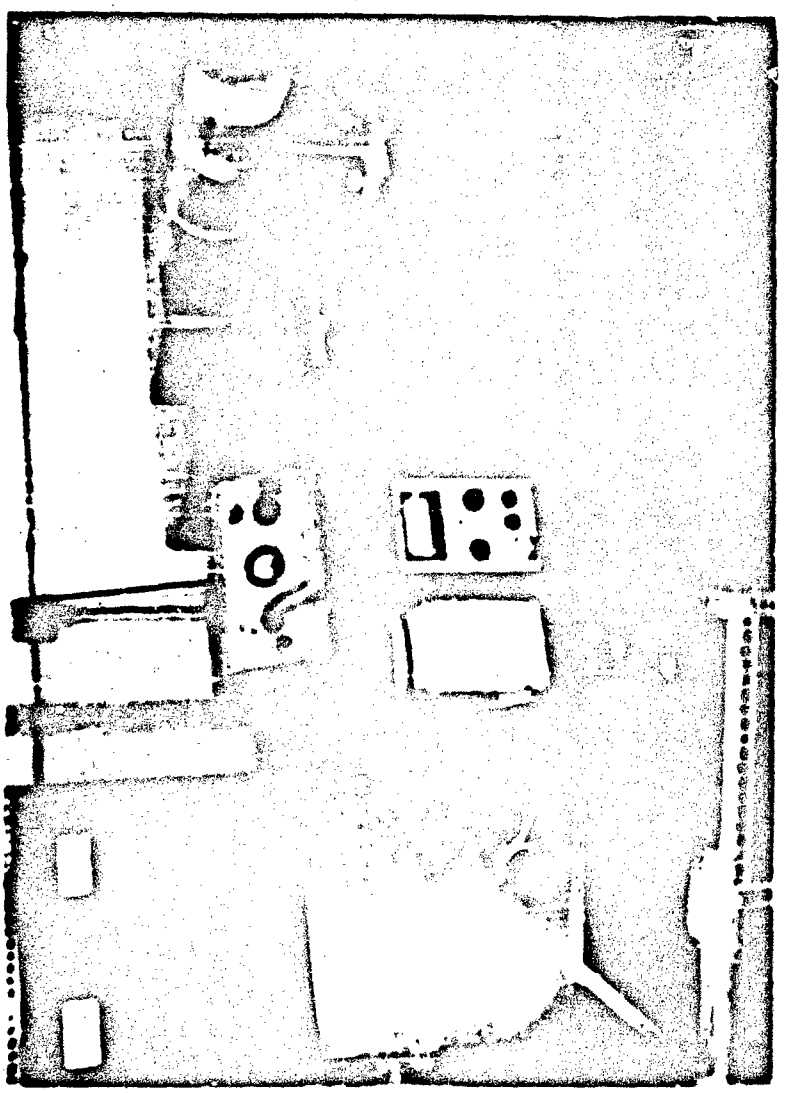

Figure 5. Experimental Setup for Energy Measurements

UNCLASSIFIED

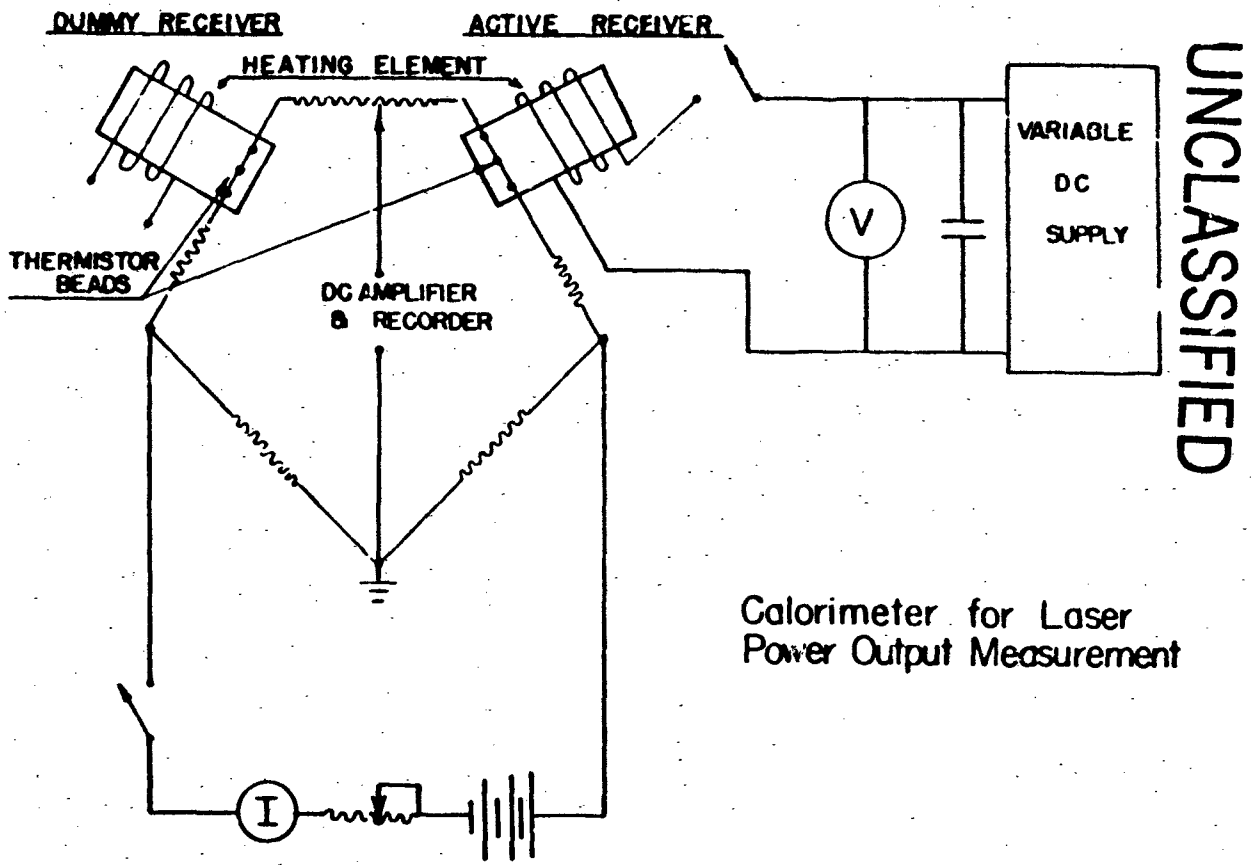

Calorimeter for Laser Power Output Measurement

Figure 6

UNCLASSIFIED

brated by putting a pulse of known energy through the platinum heating wires wrapped around the cups. The circuit diagram is shown in Figure 6.

4.1.2 FT-524 Helical Flash Tube Cavity

Initial measurements were made with a helical flash tube surrounded by a cylindrical reflector. The arrangement consists of an FT-524 helical flash tube, and a reflector of lightly packed c.p. grade magnesium oxide between an aluminum outer shell and the fused quartz cylinder surrounding the flash tube.

4.1.3 Threshold and Energy Data Obtained with the FT-524

Threshold data taken by the method described in Section 4.1.1 are given in Table 1 for Nd doped $CaWO_4$. Table 2 gives data for Nd doped glass, and table 3 gives the results for ruby. The $CaWO_4$ (Nd^{3+}) crystals were grown at Isomet, while the Nd glass and ruby rods were obtained from outside vendors. All of the rods were ground, polished and coated at Isomet.

4.1.4 Analysis of Data Obtained with the FT-524

From the data given in Table I for Nd^{3+} doped calcium tungstate we can compute a mean lasing threshold of 16.5 joules. The mean value of the threshold given in Table 2 for Nd doped glass is 455 joules, and the mean value of the threshold given for ruby in Table 3 is 1169 joules.

The results of energy measurements are plotted in Figure 7. The computed pumping efficiency is .02% for ruby and .19% for $CaWO_4$ (Nd^{3+}). The pumping efficiency was calculated using the following formula:

$$\text{Pumping Efficiency} = \frac{\text{Energy Output} \times 100}{\text{Energy input} - \text{Threshold energy}}$$

where all the energy values are in joules.

4.1.5 FX-42 Linear Flash Tube Cavity (Mark 1)

The first cavity using a linear flash tube is shown in Figure 8. The laser rod was supported in a glass tube which was placed between two linear EGG FX-42 xenon flash tubes. The reflector consisted of aluminum foil wrapped around the entire assembly. This cavity gave reasonable values for threshold and pumping efficiencies. A graph showing input energy vs. output energy for various rods is given in Figure 9.

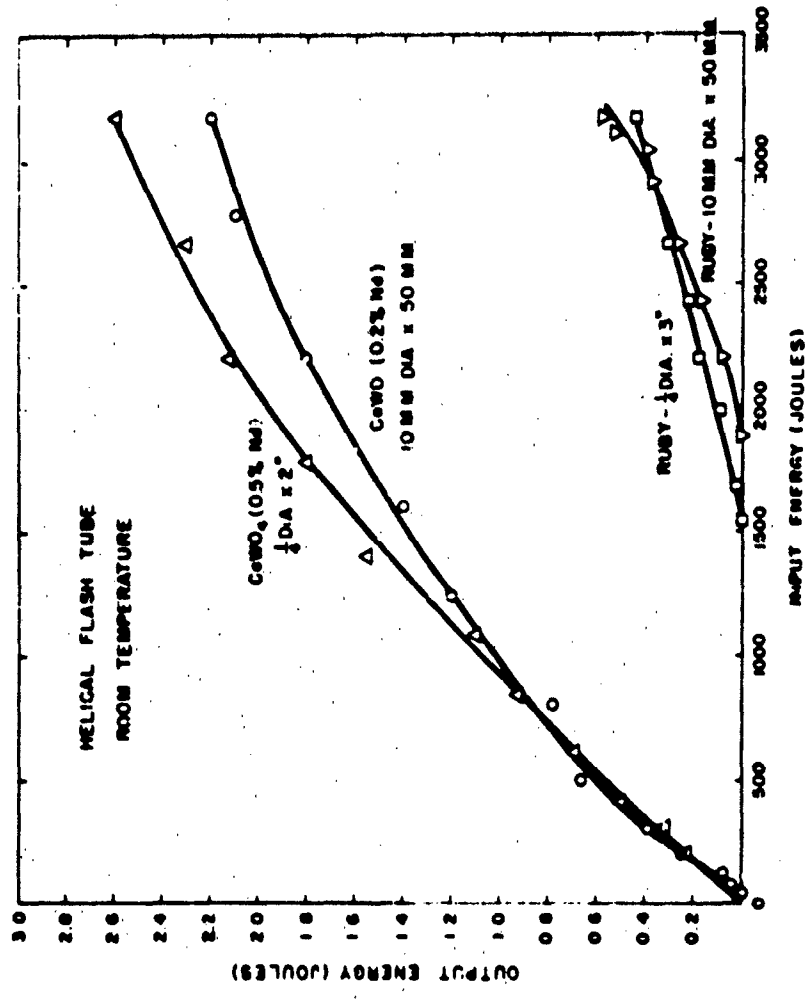

Figure 7. Output vs. Input-Helical Flash Lamp at Room Temperature

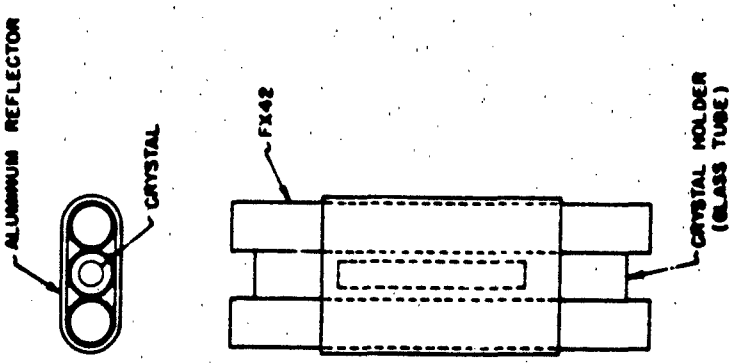

Figure 8. Linear Cavity (Mark I)

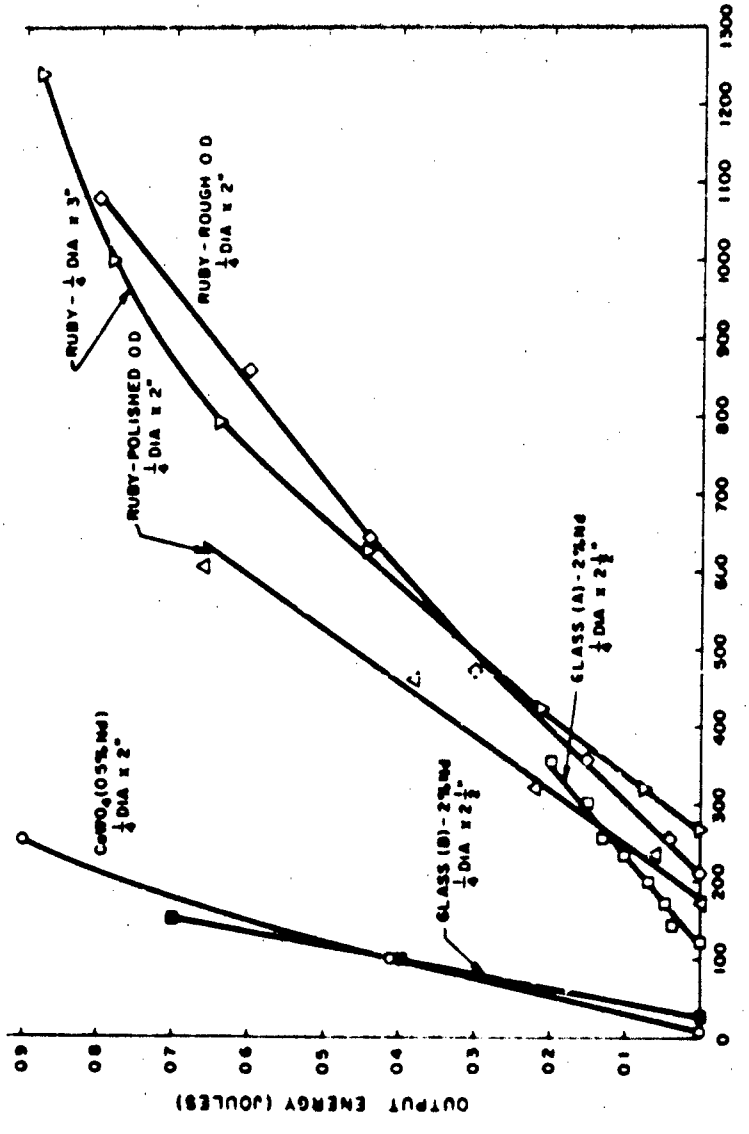

Figure 3. Output vs. Input-Linear Flash Tube at Room Temperature

TABLE 1

THRESHOLD MEASUREMENTS OF $CaWO_4$ (Nd^{3+}) LASER CRYSTALS AT ROOM TEMPERATURE IN A HELICAL CAVITY (FT524)

Sample No.	Doping	Dia. Inches	Length Inches	% T	C μf	V Volts	Energy Joules
1	.6% Nd	.250	1.833	4% D	4	3000	18
2	.6% Nd	.390	1.950	4% D	4	4400	38.7
3	.5% Nd	.250	2.000	2% D	4	3200	20.5
4	.5% Nd	.250	3.00	4% D	4.2	2100	9.2
5	.5% Nd	.250	2.00	2% D	4	2800	15.7
6	1% Nd	.250	2.00	1.5%D	4	2750	15.1
7	.5% Nd	.250	2.00	4% D	4	2700	13
8	.5% Nd	.250	2.50	3.8%D	4	2200	9.7
9	.6% Nd	.250	2.00	5% Ag	4.2	3500	25.7
10	.5% Nd	.250	2.00	1% Ag	16.7	2200	40.3
12	.5% Nd	.250	2.00	2% D	4.2	2450	12.6
13	.5% Nd	.250	3.00	1% D	4.2	2650	14.8
14	.5% Nd	.250	3.00	3.3%D	4.2	2400	12.1
15	.5% Nd	.250	2.00	3.3%D	4.2	2500	13.1
16	.5% Nd	.250	2.00	3.3%D	4.2	2250	11.2
17	.5% Nd	.250	2.00	2% D	4.26	3500	26
18	.5% Nd	.250	2.00	2% D	4.26	2200	10.3
19	.5% Nd	.250	2.00	2% D	2.2	2600	7.4
20	.5% Nd	.250	2.00	3% D	4.25	2800	16.7
22	.5% Nd	.250	2.00	3% D	4.26	3600	27.6
23	.5% Nd	.250	3.00	3% D	4.25	2400	10.4
24	.5% Nd	.250	3.00	3% D	4.25	2400	12.3
25	.5% Nd	.250	2.00	4% D	4.26	2200	10.3
26	.5% Nd	.250	2.00	4% D	4.26	2300	11.3
27	.5% Nd	.500	2.00	3% D	8.6	2700	31
28	.5% Nd	.250	1.50	2% D	4.26	2400	11.9
29	.5% Nd	.250	1.00	2% D	4.26	3800	30.8
30	.5% Nd	.250	1.93	2% D	4.26	2600	14.4
31	.5% Nd	.250	2.00	2% D	4.26	2450	12.6
32	.5% Nd	.250	2.00	2% D	4.26	2500	13.3
33	.5% Nd	.250	2.00	2% D	4.26	2600	14.4
34	.5% Nd	.250	2.00	2% D	4.26	3200	21.8
35	.5% Nd	.250	2.00	4.3%D	4.26	2300	11.3
36	.5% Nd	.250	2.00	4.3%D	4.26	2200	10.3
37	.5% Nd	.250	2.00	4.3%D	4.26	2650	14.4
38	.5% Nd	.250	1.50	4.3%D	4.26	2600	14.0
39	.5% Nd	.250	3.00	4.3%D	2.15	2800	8.4
40	.5% Nd	.250	2.00	4% D	2.15	3000	14.0
41	.5% Nd	.250	1.00	4% D	2.1½	4200	19.0

TABLE 1

(Continued)

Sample No.	Doping	Dia. Inches	Length Inches	% T	C μf	V Volts	Energy Joules
42	.5% Nd	.250	1.50	4% D	2.15	2900	9.0
43	.5% Nd	.250	1.50	4% D	4.26	3400	24
44	.5% Nd	.250	2.00	4% D	2.15	3200	11
45	.5% Nd	.200	1.00	5% Ag	4.26	4300	39
46	.5% Nd	.250	2.00	4% D	2.15	3250	11
47	.5% Nd	.250	1.00	4% D	2.15	3600	14
48	.5% Nd	.250	1.00	4% D	2.15	3400	12.4
49	.5% Nd	.125	1.875	4% D	2.15	3200	11
50	.5% Nd	.500	2.00	4% D	8.6	2600	29

TABLE 2

THRESHOLD MEASUREMENTS OF NEODYMIUM GLASS LASER CRYSTALS AT ROOM TEMPERATURE IN A HELICAL CAVITY (FT524)

Sample No.	Doping	Dia. Inches	Length Inches	% T	C μf	V Volts	Energy Joules
1	.2% Nd	.250	2.50	1.4%D	25	2800	98.0
2	.5% Nd	.250	2.00	4% D	—	—	900
3	.5% Nd	.250	2.00	4% D	—	—	850
4	.5% Nd	.250	2.00	4% D	100	3400	578
5	.5% Nd	.250	2.00	4% D	250	3400	1445
6	.5% Nd	.250	2.00	3.8%D	16.9	3300	92
7	.5% Nd	.250	2.00	3.8%D	50	3100	240
8	.5% Nd	.250	3.00	3.4%D	50	3400	289
9	.5% Nd	.250	2.00	3% D	8.6	5000	108
10	.5% Nd	.250	2.00	3% D	8.6	4500	87
11	.5% Nd	.250	3.00	3.3%D	50	3100	252
12	.5% Nd	.250	2.00	4.3%D	120	2900	505
13	.5% Nd	.250	1.00	4% D	120	3000	540

TABLE 3

THRESHOLD MEASUREMENTS OF RUBY LASER CRYSTALS
AT ROOM TEMPERATURE IN A HELICAL CAVITY (FT524)

Sample No.	Doping	Dia. Inches	Length Inches	% T	C μf	V Volts	Energy Joules
1	.05% Cr	.250	2.00	4% D	250	3800	1800
2	.05% Cr	.390	1.95	8% D	250	3800	1800
3	.05% Cr	.355	2.88	3.5%D	250	4100	2160
4	.05% Cr	.250	3.00	4% D	120	3600	886
5	.05% Cr	.250	2.00	4% D	120	3500	735
6	.05% Cr	.250	2.00	4% D	240	2500	652

The following efficiencies were calculated:

Ruby (ground o.d.)	0.085%
Ruby (polished o.d.)	0.13%
$CaWO_4(Nd^{3+})$ (ground o.d.)	0.88%

The linear arrangement shows a factor of four improvement in efficiency over the helical cavity.

Utilizing this information it was decided to design, build and test a linear cavity with more controllable parameters. The cavity (Mark 2) consisted of a 4 inch internally aluminized cylinder with a center-to-center distance between the flash tube and the laser rod of .400 inches. The laser rod was supported by a glass tube.

4.1.6 Threshold and Energy Data for Mark 2 FX-42 Cavity

Threshold data are given in Tables 4, 5, and 6 for $CaWO_4$ (Nd^{3+}), Nd doped glass and ruby.

4.1.7 Analysis of Data Obtained with the FX-42 Cavity

From the data given in Table 4 for $CaWO_4$ (Nd^{3+}) a mean value for the threshold energy of 4 joules was calculated. This is a factor of four better than obtained with the FT-524 cavity. For data given in Table 5 for Nd^{3+} doped glass we compute a mean laser threshold energy of 106 joules, which is a factor 4.5 better than that obtained with the FT-524. For two samples given in Table 6 for ruby we get an average threshold energy of 370 joules, which is a factor of 3.1 better than that obtained with an FT-524. This decrease in threshold was also evident in quality control data from a large number of laser rods which were tested in each cavity.

4.1.8 Mark 3 FX-42 Cavity

An improved version of the FX-42 linear flash tube cavity is shown in Figure 10. This cavity had the following advantages: easy access to the laser rod and flash lamp and reproducible positioning of the laser rod to 1 to 2 milliradians.

The accessibility was provided by splitting the cavity along the plane of the laser rod and flash lamp. This does not decrease the cavity performance because the radiation from the cut out portion does not reach the laser rod. The upper half of the cavity is repositioned with respect to the lower half of the cavity by the use of dowel pins.

TABLE 4

THRESHOLD MEASUREMENTS OF $CaWO_4$ (Nd^{3+}) LASER CRYSTALS AT ROOM TEMPERATURE[4] IN A LINEAR CAVITY (FX-42). CRYSTAL IN GLASS SHIELD.

Sample No.	Doping	Dia. Inches	Length Inches	% T	C μf	V Volts	Energy Joules
1	.5% Nd	.250	2.00	4% D	2.15	1900	3.9
2	.5% Nd	.250	3.00	4% D	2.15	2000	4.3
3	.5% Nd	.150	2.00	2% D	2.15	1875	3.8
4	.5% Nd	.238	2.00	4% D	4.26	1350	3.9
5	.5% Nd	.238	2.00	4% D	4.26	1300	3.6
6	.5% Nd	.250	2.00	4% D	4.26	1500	4.8
7	.5% Nd	.250	2.00	4% D	4.26	1300	3.6
8	.5% Nd	.250	2.00	4% D	4.26	1350	5.1
9	.5% Nd	.250	2.00	4% D	4.26	1350	3.9
10	.5% Nd	.250	2.00	4% D	4.26	1150	2.8
11	.5% Nd	.250	2.00	--	4.26	1250	3.3
12	Nd	.250	2.00	12%D	8.60	1000	11
13	Nd	.250	1.50	4% D	8.60	1000	4.3
14	Nd	.25	2.00	1% D	4.26	1200	3.1
15	.5% Nd	.250	2.00	4% D	4.26	1200	3.07
16	.5% Nd	.500	2.00	6% D	4.26	1800	7
17	.5% Nd	.062	1.75	6% D	2.15	1800	3.5
18	.5% Nd	.250	1.00	6% D	4.26	2200	10
19	.5% Nd	.250	1.00	2% D	4.26	2200	10
20	.5% Nd	.125	1.00	4% D	4.26	1600	5.5
21	.5% Nd	.116	1.00	4% D	4.26	2000	8

TABLE 5

THRESHOLD MEASUREMENTS OF NEODYMIUM GLASS AT ROOM TEMPERATURE IN A LINEAR CAVITY (FX-42). CRYSTAL IN A GLASS SHIELD

Sample No.	Doping	Dia. Inches	Length Inches	% T	C μf	V Volts	Energy Joules
1	2% Nd	.250	2.00	1% D	240	1200	173
2	2% Nd	.250	2.00	1% D	120	1200	86.5
3	2% Nd	.250	2.00	4% D	120	1000	60

TABLE 6

THRESHOLD MEASUREMENTS OF RUBY AT ROOM TEMPERATURE IN A LINEAR CAVITY (FX-42). CRYSTAL IN A GLASS SHIELD

Sample No.	Doping	Dia. Inches	Length Inches	% T	C μf	V Volts	Energy Joules
1	.05%Cr	.250	2.00	4% D	240	2100	530
2	.05%Cr	.250	2.00	4% D	240	1400	275

UNCLASSIFIED

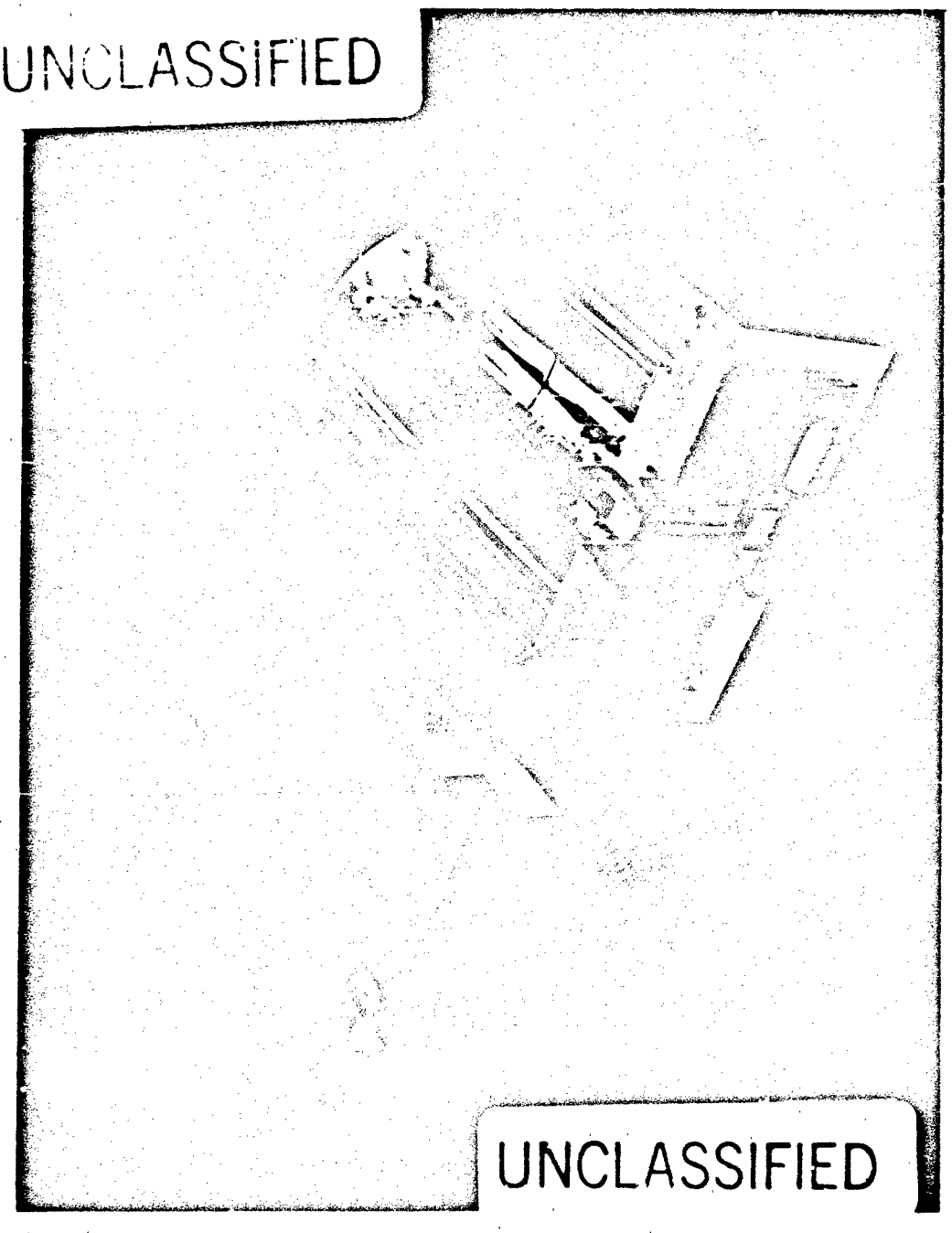

UNCLASSIFIED

Figure V. Improved Linear Cavity

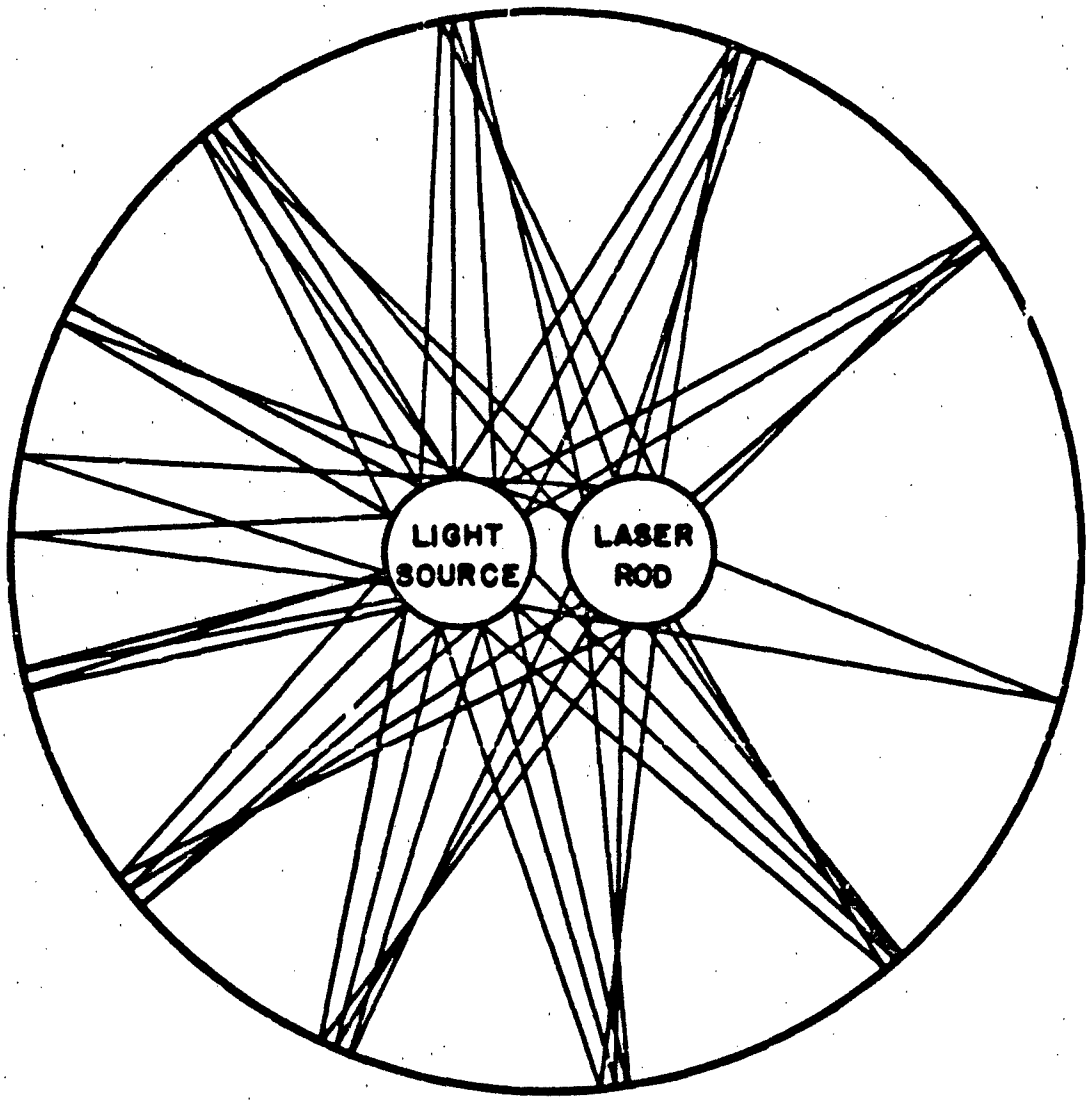

Figure 11. Ray Tracing for Cylindrical Cavity with close spacing

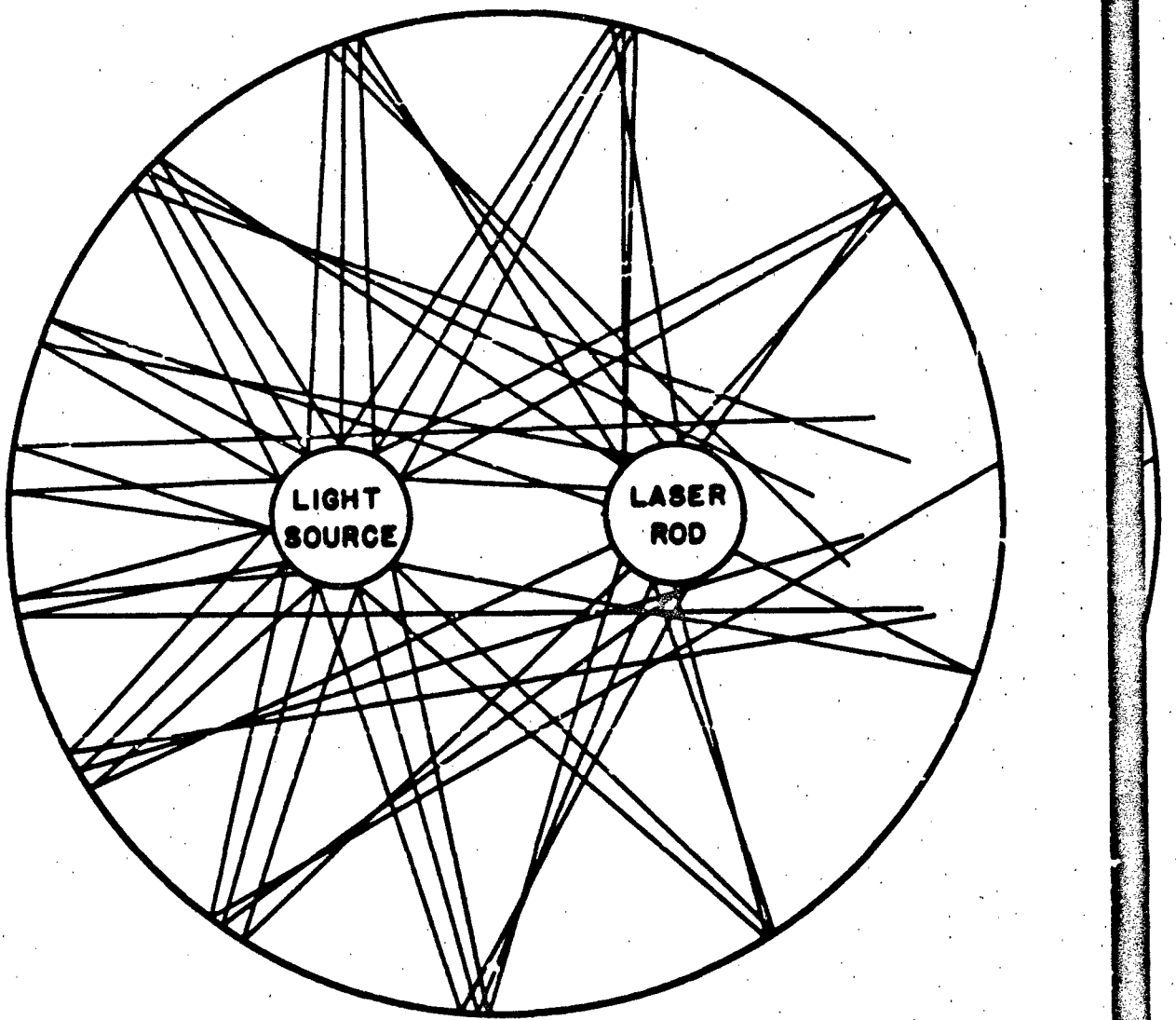

Figure 12. Ray Tracing for Cylindrical Cavity with large spacing

The laser rod was held in place by means of "V" blocks and spring clamps. The original spring clamps consisted of two phosphor bronze strips about 0.118 inches wide. In order to reduce the shielding produced by these clamps, they were replaced by .020 inch wire clamps, and the "V" blocks were ground down to reduce the shielding.

The inside diameter of the cavity was 4.00 inches and the center-to-center spacing between the laser rod and the flash lamp was 0.50 inches. These dimensions were determined by a geometrical ray trace analysis. Examples of this trace are shown in Figure 11 for the case of small center-to-center spacing, and in Figure 12 for large center-to-center spacing. In general it was found that large cavity diameter relative to the flash lamp and laser rod diameters and their separation produced the highest value of optical coupling.

4.1.9 Threshold Data Obtained with Mark 3 Cavity

Table 7 gives threshold data obtained for $CaWO_4(Nd^{3+})$, Nd^{3+} doped glass and ruby. These data were obtained for various production rods made and tested at Isomet as well as for the standard laboratory stock of test lasers.

The mean threshold energy for the three $CaWO_4(Nd^{3+})$ laser rods was 4.0 joules. The single Nd doped glass laser rod had a threshold of 14 joules. This was the lowest threshold found for an Nd doped glass rod. The two ruby rods had an average threshold of 445 joules. The elimination of the glass tubing should yield a slight decrease in the threshold energy requirement.

4.1.10 Effect of Using an FX-38A Xenon Flash Tube Instead of the FX-42

In the optical ray trace analysis of laser cavities, it became apparent that the diameter of the flash tube should be equal to or smaller than the laser rod for most efficient optical coupling. The smaller the diameter of the flash tube the better the coupling.

Data taken using the FX-38A flash tube is given in Table 8 for $CaWO_4(Nd^{3+})$ and ruby. The ruby rod had a threshold of 173 joules, while the same rod had a threshold of 308 joules with the FX-42 flash lamp. This is an improvement of 1.8 in threshold. The $CaWO_4$ (Nd^{3+}) data give a mean value of 2.2 joules for laser threshold and a minimum threshold of 1.5 joules was obtained. This would indicate a factor of 2 improvement over the FX-42 in laser threshold energy.

TABLE 7

THRESHOLD MEASUREMENTS OF UNSHIELDED RUBY, NEODYMIUM GLASS AND $CaWO_4$ (Nd^{3+}) CRYSTALS AT ROOM TEMPERATURE. FS-42 FLASH TUBE.

Sample No.	Doping	Dia. Inches	Length Inches	% T	C μf	V Volts	Energy Joules
$CaWO_4$							
1	.5% Nd	.250	2.00	5.5%D	8.6	1200	6
2	1% Nd	.250	2.00	4% D	2.15	1800	3
3	.5% Nd	.250	2.00	4% D	2.15	1800	3
Nd Glass							
1	.5% Nd	.250	3.00	4% D	8.6	1800	14
Ruby							
1	.05%Cr	.250	2.00	4% D	16	1950	308 polished O.D.
2	.05%Cr	.250	3.00	2% D	240	2190	580 polished O.D.

TABLE 8

THRESHOLD MEASUREMENTS OF UNSHIELDED RUBY AND $CaWO_4$ (Nd^{3+}) CRYSTALS AT ROOM TEMPERATURE. FX-38A FLASH TUBE

Sample No.	Doping	Dia. Inches	Length Inches	% T	C μf	V Volts	Energy Joules
$CaWO_4$							
1	.5% Nd	.250	2.00	4% D	8.6	900	3.8
2	.5% Nd	.250	2.00	4% D	2.15	1300	1.8 Pol. O. D.
3	.5% Nd	.250	2.00	5.5%D	4.26	1300	3.6
4	.25%Nd	.125	2.00	2% D	2.15	1200	1.5
Ruby							
1	.05%Cr	.250	3.00	4% D	16	1450	173 Pol. O. D.

No data on energy output versus input energy has been taken for the Fx-38A flash tube arrangement. However, theoretical studies, and projection of the analysis of results of the comparison between the linear and helical cavities would tend to give an improvement in pumping efficiency of 2 over the FX-42 or pumping efficiencies of 3% for $CaWO_4$ (Nd^{3+}) and about 1% for ruby.

4.2 Q-Switched Lasers

4.2.1 Q-Switch Laser Analysis

Q-switched "giant" laser pulses are produced by rapidly changing the Q (quality) of the cavity from a low Q state (characterized by high losses) to a high Q state (where the loss rate is low), while the laser crystal is being optically excited. By this means the laser crystal can be pumped to high levels of inversion (where the excited state population is greated than the terminal level population) under conditions of low cavity Q. When the Q is suddenly increased, the stored energy can be released in a "giant" pulse. This effect has been demonstrated in ruby [15] and in neodymium doped glass [16] where peak power in excess of 30 megawatts have been produced in both systems. Q-switching has also recently been demonstrated for neodymium doped calcium tungstate [17]. This technique can be used with any material that exhibits normal oscillation, provided the excitation is accomplished in a time that is short compared to the normal fluorescent lifetime of the crystal. The amount of energy available in the pulse is dependent on the degree of inversion and the cavity losses at the time of Q-switching.

For example, neodymium in a host lattice of glass oscillates by absorbing energy in three main absorption bands at 28,000 cm^{-1}, 18,000 cm^{-1}, and 12,000 cm^{-1} and then falls by a radiationless transition to a level at about 11,400 cm^{-1}. Laser oscillation occurs by emission from this level to a level about 2,000 cm^{-1} (shown in Figure 13). Since the terminal laser level is 2,000 cm^{-1} above the ground state, it is relatively unpopulated

15. "Characteristics of Giant Optical Pulsations from Ruby"-F.J. McClung and R.W. Hellwarth, Proceedings of IEEE - Jan.1963 p.46
16. "Neodymium Glass Laser" Quantum Electronics Conference, 1963 Paris - E. Snitzer
17. D. Karlsons & T. Falvey, "Q-Switched $CaWO_4$-Nd^{3+} Laser" J. Appl. Physics, Vol. 34, No. 11, 1963 p. 3407

even at room temperature. This means that inversion can occur with low input power compared to three level laser systems, such as ruby, where the terminal laser level is the ground state and more than half of the ions have to be pumped into the excited state. A further advantage of Nd crystals is that the main absorption bands are sufficiently close to the laser excited level that heat generated by the radiationless transition to the excited level is smaller than in other systems. In addition, neodymium in calcium tungstate and glass has a fluorescence quantum efficiency close to 1[18], compared to ruby with a quantum efficiency of about 0.6[19].

One of the major considerations in the design of a Q-switch system is obtaining the necessary switching speeds. Figure 14 is a graphic representation of the timing requirements. At t_o the flash lamp is ignited. As the crystal is pumped, a degree of inversion is reached at which the crystal could oscillate if the cavity Q were high [$f(N)_o$]. The degree of inversion continues to increase to a maximum $f(N)_1$, [where f(N) is a function of the degree of inversion]. When this point has been reached, t_s, the aperture is lined up with the crystal and oscillation occurs. The maximum energy obtainable is that represented by $f(N)_1 - f(N)_o$. As is shown in Figure 14 there is a time after t_s during which no oscillation occurs. This is the time required for the pulse to build up and is about 150 nanoseconds. It has been shown[1] that if Q-switching is done at rates slower than this build up time, multiple pulses can develop.

At present Q-switching is accomplished by means of Kerr cells, Pockels cells or mechanical Q-switches. The latter consist of rotating total internal reflection prisms or mirrors with optical "speed doublers" or other optical devices which increase the effective switching speed. All of these devices suffer from limitations. With a Kerr or Pockels cell polarizers must be introduced into the cavity or other means found to polarize the laser beam. This introduces optical insertion losses and optical alignment difficulties. A further disadvantage is that for Kerr cell switching, up to 1/3 of the energy can be lost by conversion from the main laser frequency to Raman frequency light by the nitrobenzene in the Kerr cell. As far as rotating prisms and optical "speed doublers" are concerned, they introduce alignment problems and insertion losses in addition to increasing the opti-

18. "Characteristics of $CaWO_4(Nd^{3+})$ Optical Maser" - L.F. Johnson Quantum Electronics Conference 1963 - Paris
19. "Laser Materials and Devices - A Research Report," R.D. Haun, Electro-Technology, September 1963, p. 67.

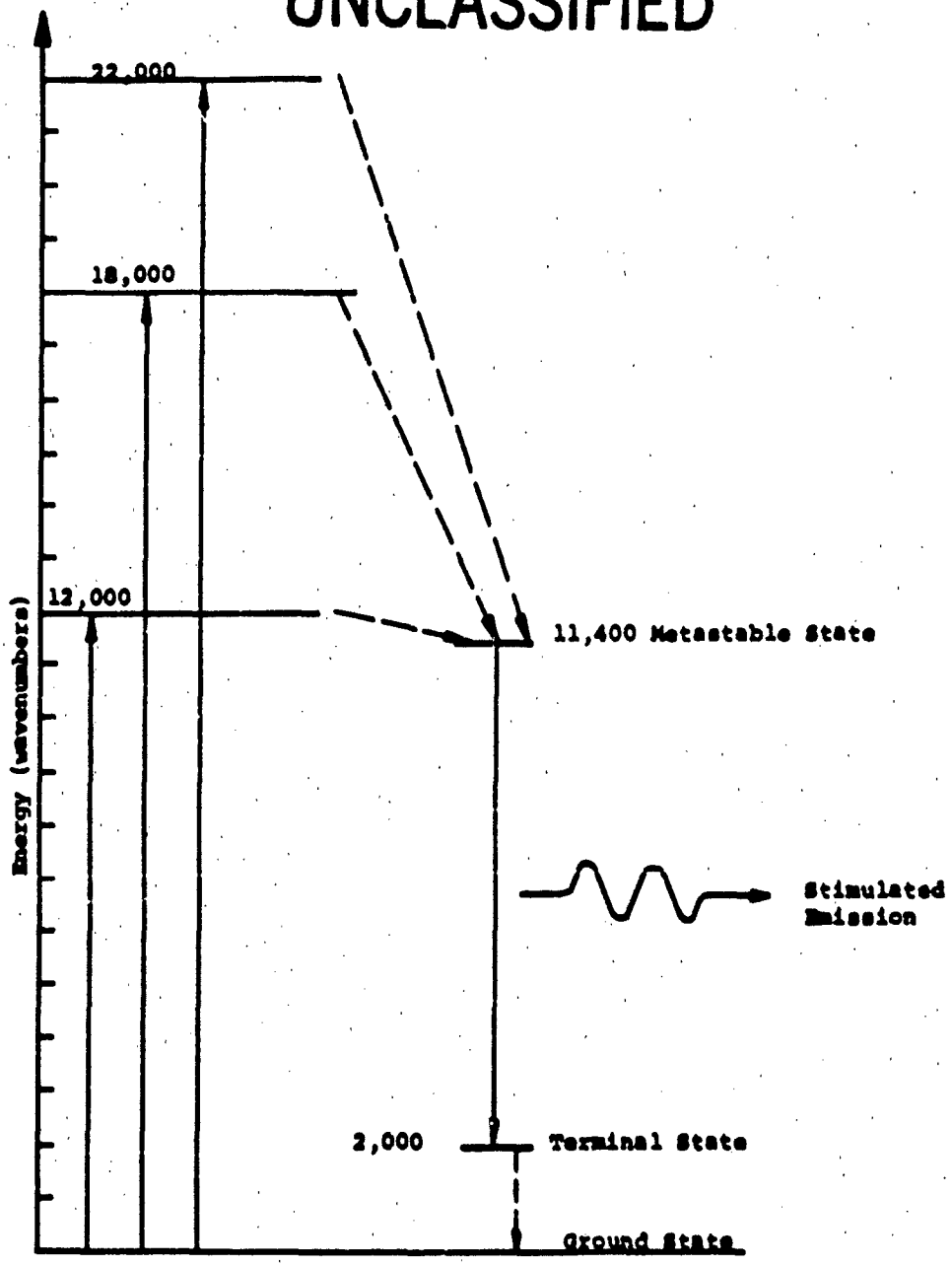

Figure 13. Four level laser

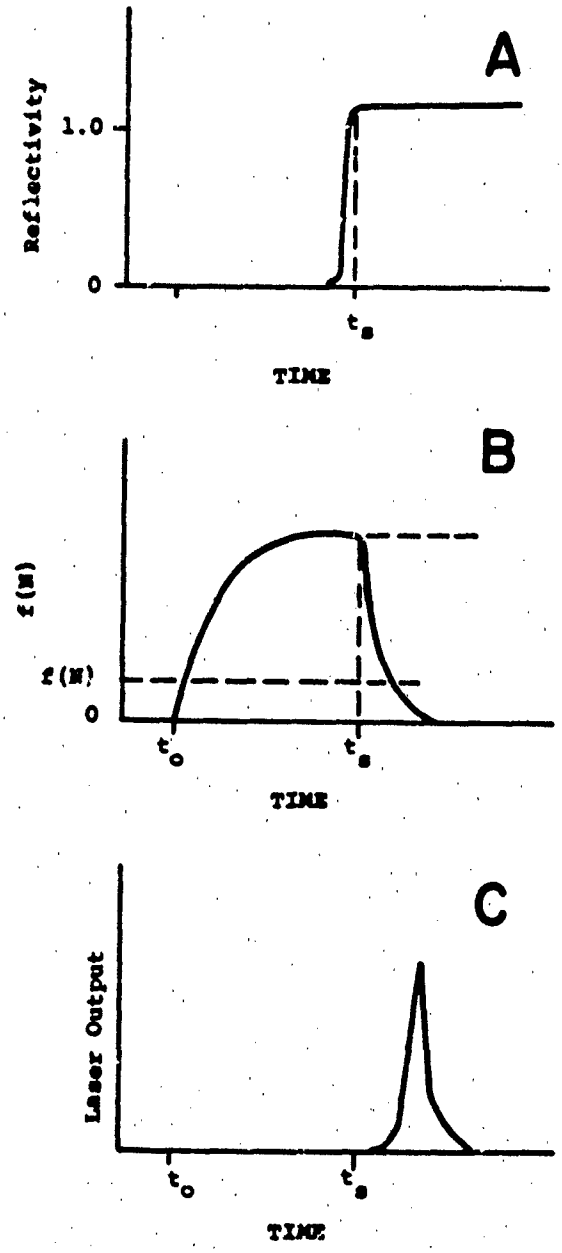

Figure 14. Laser Timing Requirements

cal path length of the cavity and thereby increasing the pulse width. Each of these techniques has been critically examined. A mechanical chopper-telescope combination has been developed that offers high efficiency and reliability.

4.2.2 Damage to Optical Elements

The high peak power developed in Q-switching produces extremely high power densities that can lead to the destruction of mirrors, reflective coatings and optical elements. It is planned to overcome this problem by the use of a proprietary technique developed at Isomat that employs the use of optical elements within the laser cavity to increase the laser beam diameter. This technique, in addition to providing mode selection, distributes the high peak power from the laser over a larger area thus contributing to a marked increase in life expectancy of the system.

4.2.3 Kerr Cell Q-Switching of Ruby

4.2.3.1 Experimental Arrangement Used in Kerr Cell Q-Switching of Ruby

A schematic drawing of the experimental arrangement used in this series of experiments is shown in Figure 15. The laser cavity was of the FT-524 helical flash tube type. With this cavity the threshold for the ruby laser rods ranged from 694 to 1200 joules. The polarizer consisted of a Nicol prism. The Kerr cell used in these experiments was a Kappa Series 8 using nitrobenzene as the working fluid. The cell was anti-reflection coated for 6943A. Minimum transmission occurred at 31 kilovolts. The Kerr cell was pulsed by a KV-27 low inductance thyratron, and powered by 34 KV variable power supply.

4.2.3.2 Experimental Results Obtained

Considerable problems were encountered in using the Kerr cell as a Q-switch. Initially, voltage breakdown and corona discharge produced inconsistent results. More insulation was added to the pulser eliminating most of the breakdown problems.

The Q-switch still performed poorly. Measured output pulses of several hundred KW were produced. An open to closed transmission ratio of only 7.5:1 was obtained, which explains to some extent the poor performance as a Q-switch. For high performance it would be necessary to use ultrapure nitrobenzene and more efficient polarizers, and to anti-reflection coat all surfaces. The use of Brewster angle ends on the ruby would also help to increase power output. At this time it was decided that a mechanical

UNCLASSIFIED

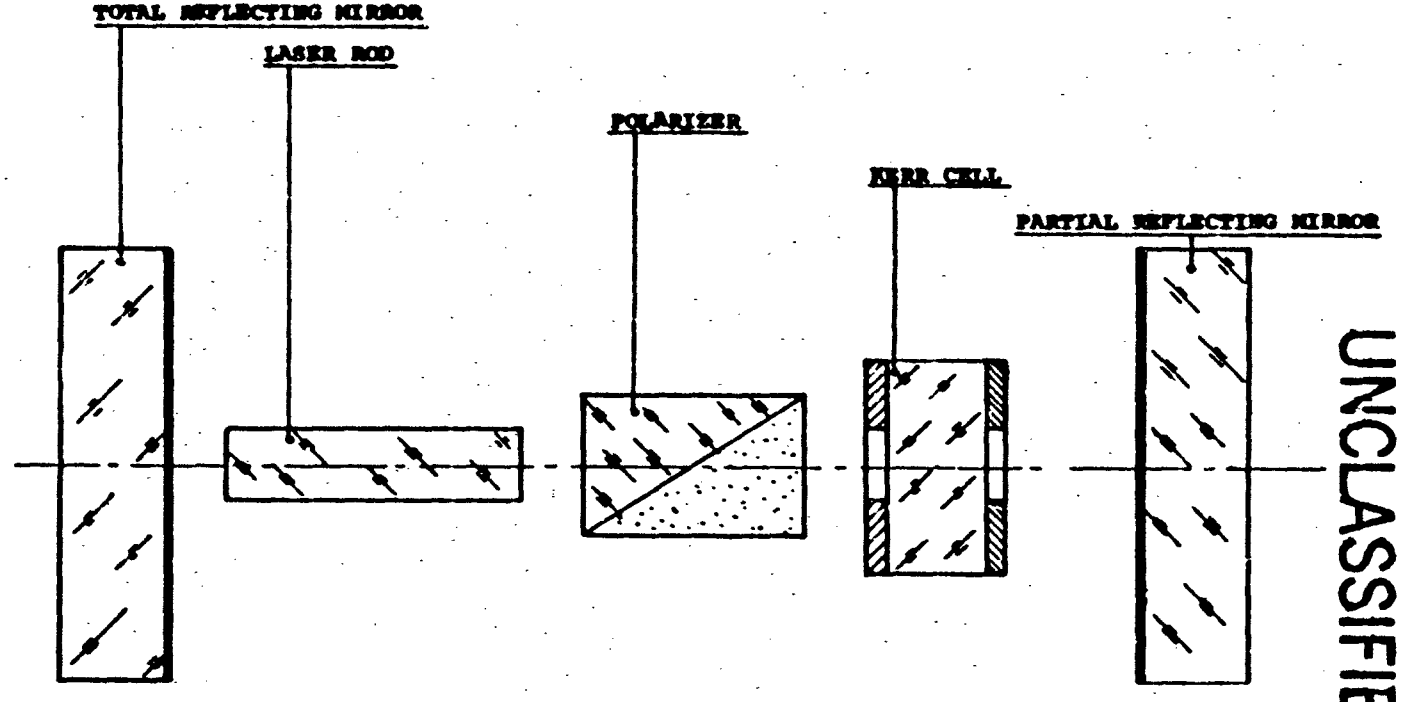

FIGURE 15 - EXPERIMENTAL "Q" SWITCHED LASER ILLUMINATING SYSTEM

UNCLASSIFIED

UNCLASSIFIED

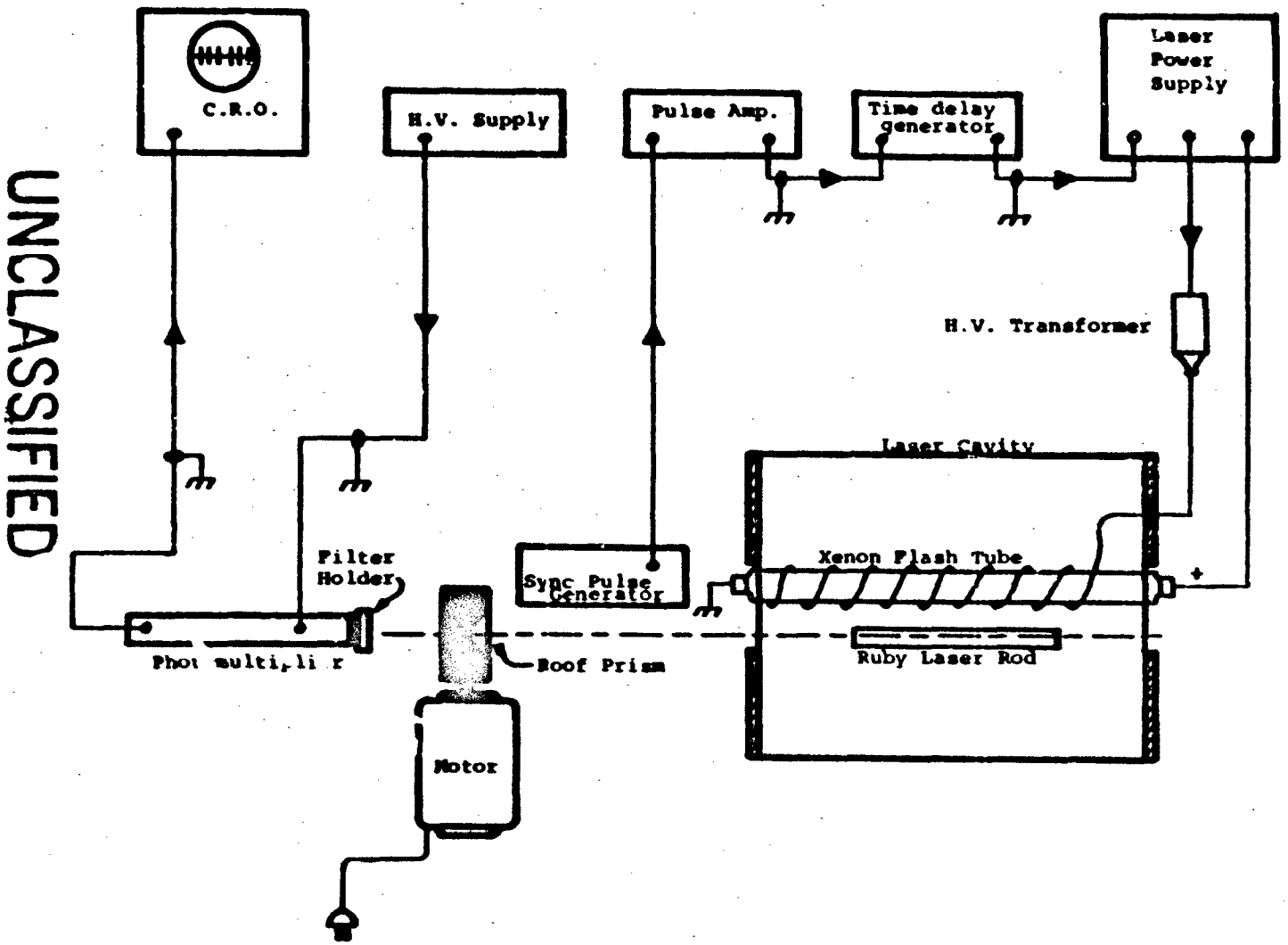

Figure 16. Mechanical Q-Switch Assembly

UNCLASSIFIED

UNCLASSIFIED

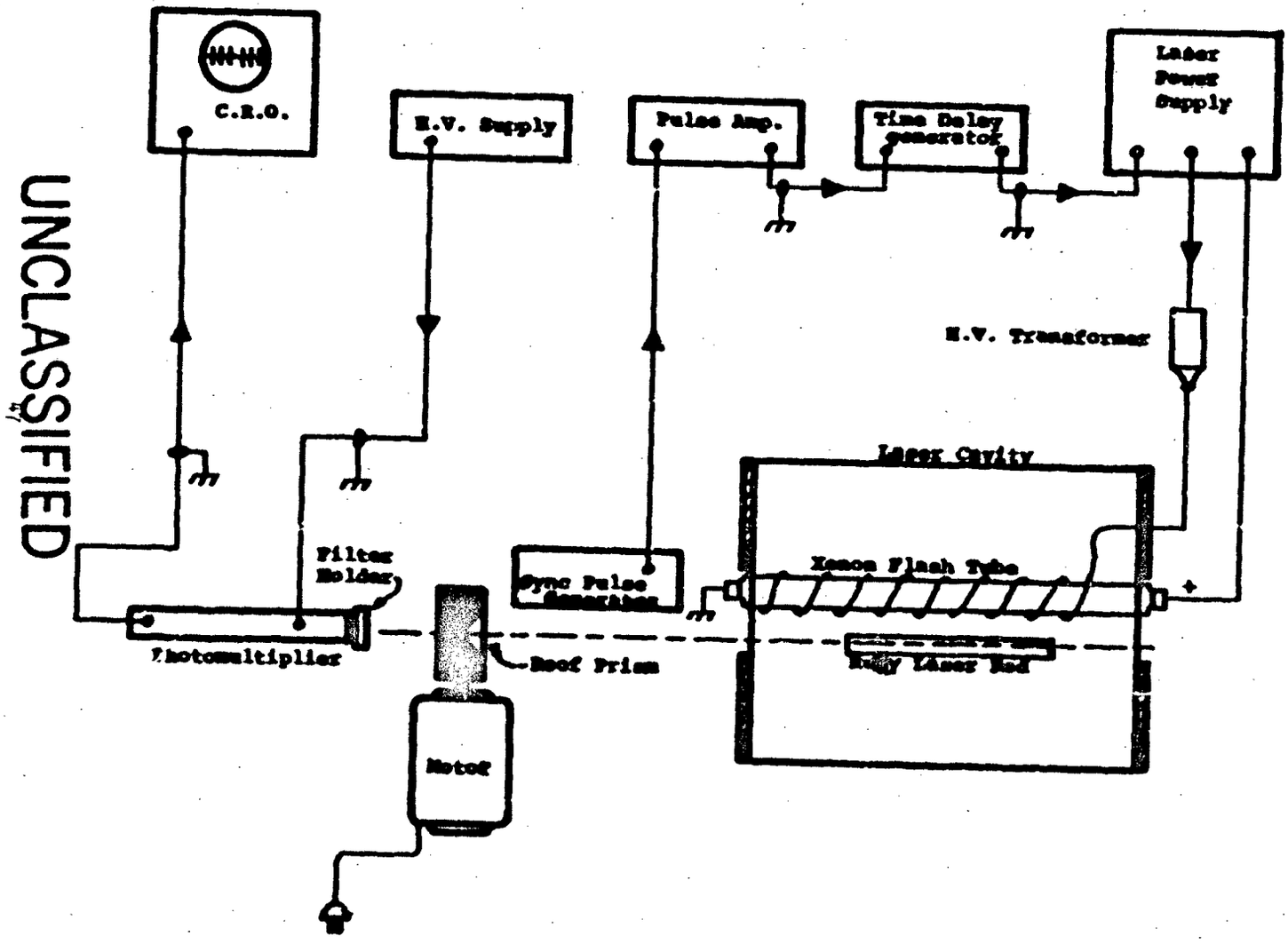

Figure 16. Mechanical Switch Assembly

UNCLASSIFIED

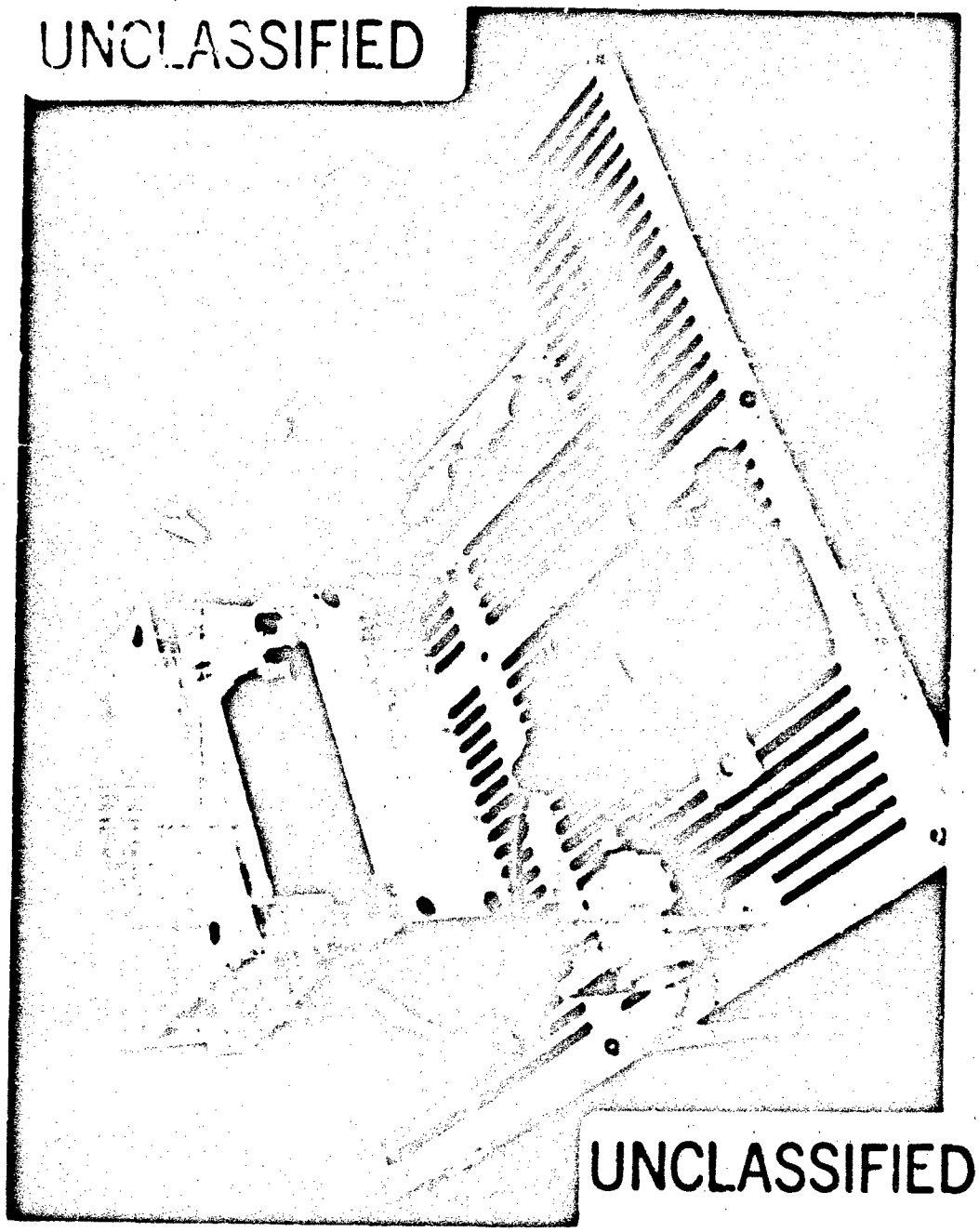

Figure 17. Mechanical Q-Switching Assembly

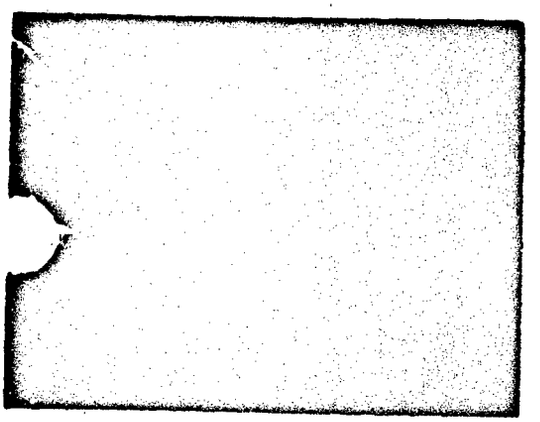

Ruby Q-Switched Output
1 microsecond/cm

Figure 10

Q-switch would provide more reliable operation at higher peak powers, and no further work with Kerr cells was carried out.

4.2.4 Mechanical Q-switch

A mechanical Q-switch was fabricated using a 17,500 rpm universal wound motor driving a 90° prism. After some initial alignment problems excellent performance of this Q-switch was obtained.

4.2.4.1 Experimental Arrangement Used in Mechanical Q-Switching

A schematic diagram of the mechanical Q-switching setup is shown in Figure 16, while Figure 17 shows a photograph of this arrangement. The cavity utilised an EGG FX-42 xenon flash tube with a glass tube to support the laser rod. The motor speed was 17,500 rpm. The prisms used were 90° TIR (total internal reflecting). In some of the prisms the roof edge was polished to permit monitoring the output on both sides of the cavity. A phototransistor and a small light bulb were used to fire the flash lamp. The output from the phototransistor was fed to an Abtronics Model 200 two channel time delay generator, in order to vary the time when the flash lamp was fired so as to secure the maximum output.

4.2.4.2 Experimental Results

Figure 18 shows a photograph of a typical output pulse resulting from Q-switching with an input energy of 975 joules. The trace was taken with an EGG SD-100 photodiode as the sensor. The decay time of the pulse is limited by the interconnecting cable capacity. The calibration of the photodiode gave a sensitivity at the ruby wavelength of 0.55×10^{-2} v/watt. The diode

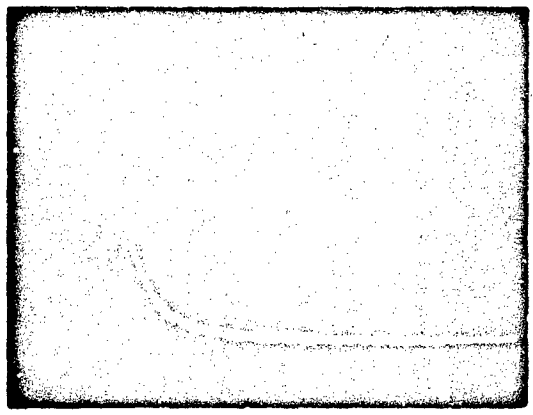

$CaWO_4:Nd^{3+}$ - Normal Laser Output
5 microsecond/cm

$CaWO_4:Nd^{3+}$ - Q-Switched Laser Output
10 microsecond/cm

Figure 11. Pulse Shape of $CaWO_4$ (Nd^{3+}) for Q-Switched and Normal Laser

was located at a working distance of 6 inches from a magnesium oxide reflector having a reflectivity of 0.92. The peak output power was calculated to be of the order of 7 megawatts in a single pulse. Some difficulty was encountered in making these measurements because the oscilloscope used was rise time limited. It is likely that the pulse voltage was actually greater than shown in the photograph; the output power would accordingly be greater than 7 megawatts.

4.2.4.3 Attempted Q-Switching of Calcium Tungstate (Nd^{3+})

Attempts were made to Q-switch calcium tungstate. The metastable state lifetime for $CaWO_4$ (Nd^{3+}) is much shorter than that for ruby so that any errors or variations in timing caused large changes in the output pulse amplitude. At the rotational speeds of the Q-switching prism, a timing accuracy equivalent to 2° of prism rotation were required. The setup did not have this degree of precision. Figure 19 is an illustration of one of the Q-switched outputs. For comparison the normal laser output is also shown. Quantitative data could not be obtained because of timing jitter.

4.2.5 Second Harmonic Generation Experiments

Using KDP as second harmonic generation material, some experiments were conducted on second harmonic generation with a mechanical Q-switch and a ruby laser. The results were inconclusive, since the high peak power of the laser resulted in the destruction of the crystal.

At this time very promising results were obtained with infrared stimulable and infrared emitting phosphors. Since an IR-IR system is more efficient than a UV-IR system (because an energy loss of at least five in harmonic generation is avoided) it was decided to discontinue second harmonic studies.

4.2.6 Optical Damage Encountered

A series of experiments were performed to determine the effect of Q-switched laser beams on optical elements. In each case a focussed ruby laser beam of approximately 7 megawatts peak energy was directed into the material. The following results were observed:

a. Lucite block - showed bubbles where laser beam went

through.

b. KDP - Showed bubbles and fracture marks where beam went through.

c. Prism - Surface pitted by beam.

d. Cemented Positive Achromatic Lens - Cement destroyed, glass pitted at exit side.

e. Dielectric coatings - Destruction after one or more laser pulses.

4.2.7 High Repetition Rate Lasers

Many lasers have been operated continuously. Solid State crystal lasers such as neodymium doped calcium tungstate can be operated continuously at room temperature, if water cooled (18,20). Calcium tungstate, ruby and other materials have been lased continuously at liquid nitrogen temperatures[18]. It is, therefore, reasonable to expect that a laser such as $CaWO_4(Nd^{3+})$ can be pulsed at a high repetition rate provided that an efficient cavity and cooling are used and a high rep rate efficient pump is available. This, fortunately, is not an insurmountable problem.

Considerable advances are being made in flash lamps. In the past six months the average flash tube power has been raised from 20 watts for an FX-38A and 60 watts for an FX-42 to 4,000 watts for an FX-62. The FX-42 and FX-62 are almost identical in optical dimensions. The FX-62 can be fired at 50 pulses per second, while the FX-42 has a maximum rep rate of one per ten seconds.

One promising direction being developed at Isomet involves the use of a sodium vapor lamp as the pump source. Figure 20 shows the absorption spectra of Nd^{3+} and the emission spectra of sodium. Numerical computation indicates a possible 50 fold improvement in pump efficiency.

4.2.8 Thermal Heating at High Rep Rates

The temperature rise for xenon pumping can be computed for the following conditions:

a. A water jacket is used to eliminate the infrared radiation.

---

20. L.F. Johnson, G.D. Boyd, K. Nassau and R.R. Soden "Continuous Operation of a Solid State Optical Maser." Phys. Rev. 126,1406 (1962).

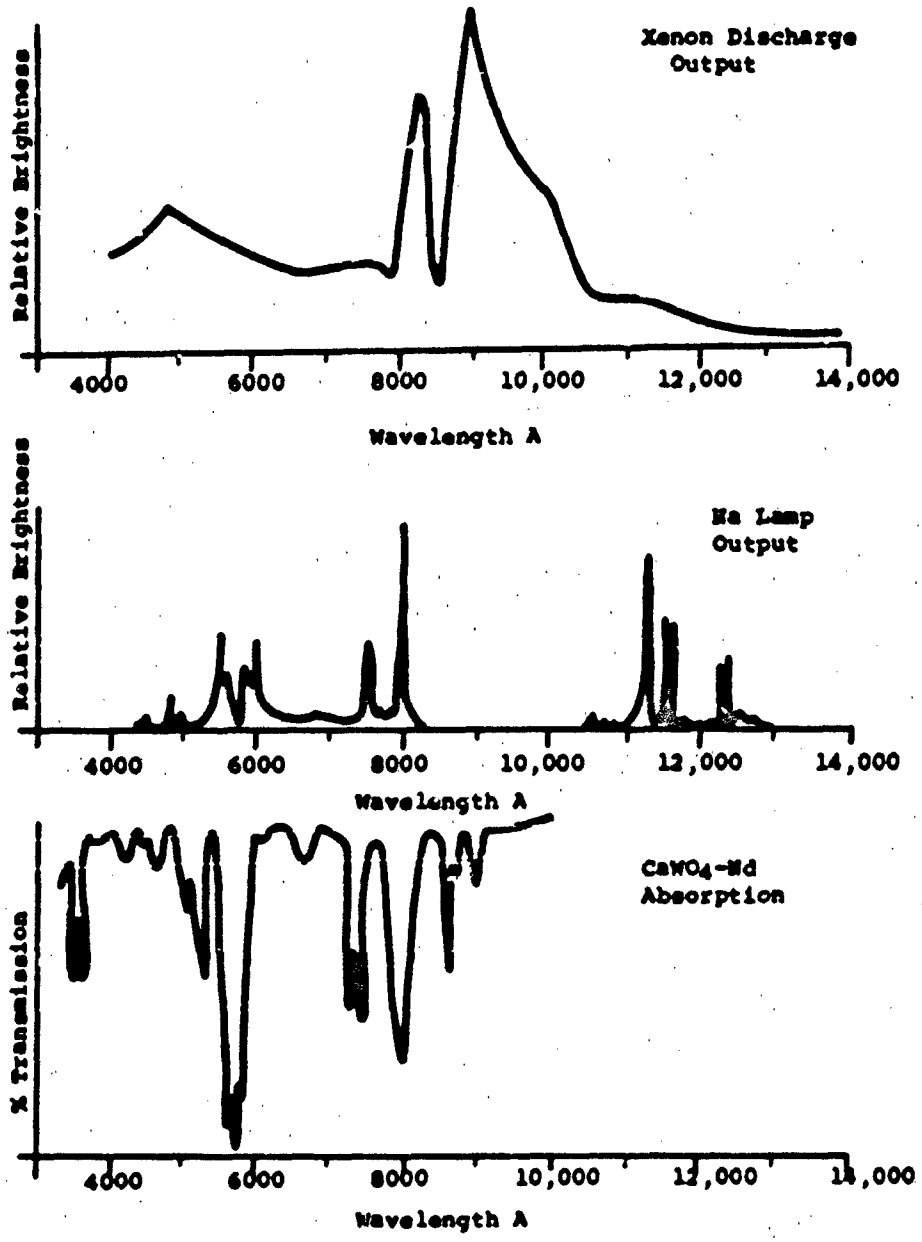

Figure 20. Lamp Emission Spectra and Neodymium Absorption Spectra

b. 70% of the radiant output of the lamp is focussed at the crystal, as a result of high coupling efficiency in the cavity.

c. 8% of the energy focussed on the crystal is absorbed by the dopant with a quantum efficiency of 100%.

Hence:

$$\text{Temperature rise} = \frac{\text{Energy Absorbed}}{\text{Volume} \times \text{density} \times \text{specific heat}}$$

$$= \frac{10 \times .08 \times 0.7 \times 0.24}{2.3 \times 6.06 \times 0.104}$$

$$= 0.09^{\circ}\text{C/pulse}$$

Although the temperature rise is small, at 50 pps this corresponds to 2.1 cal/sec.

The cooling requirements can be estimated from the conductivity equation:

$$\frac{dQ}{dt} = -K A \frac{d\theta}{dx}$$

where dQ/dt = rate of heat transfer
K = coefficient of thermal conductivity
A = area
$d\theta/dx$ = temperature gradient

Assuming a rectangular cross section laser rod the estimated thermal gradient will not exceed 30° above ambient. Using air as the coolant 3 cu ft of air/minute will limit the temperature rise at the surface to 0.5°C above ambient. This is sufficient cooling to keep the laser oscillating at a high level. The computed max thermal gradient is not high enought to seriously strain the crystal.

4.3 Photometer

A photometer was constructed and used to measure the infrared emission for all of the phosphor samples. A sketch of this basic device is shown in Figure 21.

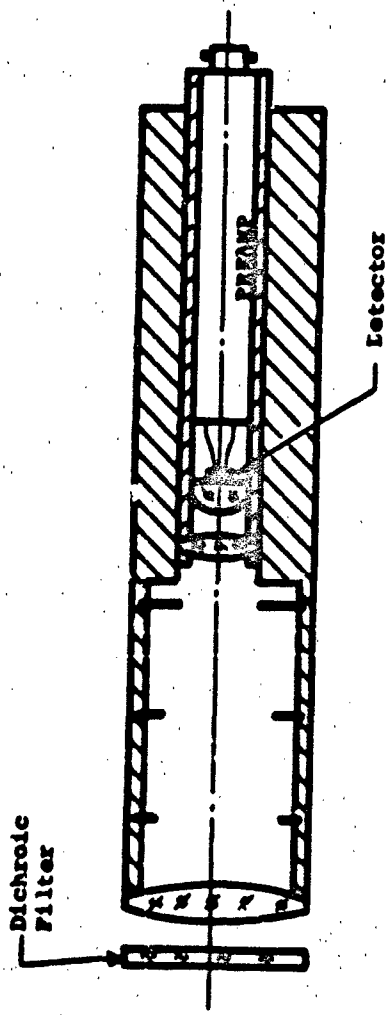

Figure 21. Photometer Head

The field lens was adjusted so that the device exhibited a relatively flat sensitivity curve as a function of angle of source for the three degree field. Therefore, aiming of the photometer was not critical.

The sensitivity of the photometer, was found to be 0.48 volts per microwatt of incident light of wavelength 1.06 microns. The spectrum of a calibrated incandescent lamp was filtered by a KDP crystal and an Isomet 718-B interference filter.

The detector was a PbS cell with a rated detectivity of 9×10^{8} watts-cm$(cps)^{1/2}$ and is capable of measuring radiation power densities as low as 5×10^{-11} watts/cm^2.

4.4 Phosphor Studies

4.4.1 Phosphor Preparations

4.4.1.1 Exploratory Phosphors

Initially a series of phosphors were prepared and examined for emission in the infrared using a 3470A excitation source. The phosphors were prepared by mixing a quantity of the host (such as ZnS or CdS) with a few ml of a solution of the activator ion. A small quantity of NaCl was also added. The suspension was dried pulverized and fired in air in an aluminum oxide crucible at 900°C for one hour. Table 9 shows a list of phosphors that were prepared in this manner. CdS(Cu,Tl,Cl) and CdS(Cu,Tb,Cl) were found to be useful phosphors with strong infrared emission. The other phosphors in Table 9 did not show any infrared emission within the range of the detector, (1.3 to 2.6 microns).

Another series of phosphors was prepared in a similar manner but was examined for infrared emission when excited with 1.06 micron radiation. Table 10 lists the phosphors prepared along with their relative radiant efficiency. CdSe was found to be a promising host.

The high radiant efficiencies displayed by these IR stimulated and IR emitting phosphors, along with the highly efficient 1.06 micron laser excitation source made possible by $CaWO_4(Nd^{3+})$ or neodymium glass, prompted a decision to concentrate efforts on IR-IR phosphors. ZnS, and CdS and CdSe doped with various heavy metals were selected as promising phosphor system. Careful preparations and studies were made with these materials.

TABLE 9

LIST OF POTENTIALLY USEFUL PHOSPHORS SYNTHESIZED

No.	Sample	Composition	Radiant Efficiency
1.	1	(Zn,Cd)S;Cu	*
2.	2	$CaWO_4$(Nd)	0.2%
3.	3	(Zn,Cd)S,Cu [NaCl]	*
4.	4	(Zn,Cd)S:Cu [NaCl]	*
5.	5	CdS:Cu:Tl [NaCl]	*
6.	6	CdS:Cu:Tl [NaCl]	1.2%
7.	7a	CdS:Cu:Tl(.1) [NaCl]	*
8.	7b	CdS:Cu:Tl(1) [NaCl]	*
9.	7c	CdS:Cu:Pb(0.1) [NaCl]	*
10.	8	CdS:Cu:Sn [NaCl]	*
11.	8a	CdS:Cu:Co [NaCl]	*
12.	8b	CdS:Cu:Ni [NaCl]	*
13.	8c	CdS:Cu:Tb(.05) [NaCl]	1.8%
14.	9	PbS:Ag:Tb [NaCl]	*
15.	9a	PbS:Cu:Tb [NaCl]	*
16.	10	CdS:Ag [NaCl]	*
17.	10a	CdS:Ag:Tb [NaCl]	*
18.	10b	CdS:Cu:Tb [NaCl]	*
19.	11	ZnS:Cu:Al [NaCl]	*
20.	11a	ZnS:Cu:Co [NaCl]	*
21.	11b	CdS:ZnS:Cu:Tb [NaCl]	*
22.	12	CuS:Tb [NaCl]	*
23.	12a	CuS:Ag [NaCl]	*
24.	12b	CuS:Co [NaCl]	*

* No IR Output observed

TABLE 10

LIST OF POTENTIALLY USEFUL PHOSPHORS SYNTHESIZED

	Sample No.	Composition	Firing Temp. °C	Relative Radiant Efficiency
1	Standard	CdSe:Cu:In	1000	.0100
2	14a	CdSe:Cu:Dy [NaCl]	800	.0020
3	14b	CdSe:Mn [NaCl]	800	.0037
4	16	CdS:Cu:In [NaCl]	800	.0045
5	17	CdSe:Cu:In [NaCl]	800	.0078
6	17a	CdSe:Mn [NaCl]	800	.0054
7	17b	CdSe:Mn:Dy [NaCl]	800	.0032
8	17c	CdSe:Mn:In [NaCl]	800	.0040
9	18	*Cd(Se,S);In:Cu [NaCl]	700	.0340
10	18a	*Cd(Se,S)In:Cu:Dy [NaCl]	700	.0400
11	18b	CdSe:In:Cu [NaCl]	800	.0100
12	19	Cd(Se,S)Cu:In:Dy: [NaCl]	700	.0180
13	19a	Cd(Se,S)Cu:In:Dy [NaCl]	700	.0075
14	19b	CdSe:Cu(Cl):In:Dy [NaCl]	800	.0030
15	20	*Cd(Se,S)Cu:Mn	600	.0065
16	20a	*Cd(Se,S)Cu:Mn	700	.0050

*Se:S ratio = 1:1

4.4.1.2 Selected Efficient Phosphors

Four particularly good infrared emitting phosphors were prepared. Two of these were tested and found to have high radiant efficiency when excited by 1.06 micron radiation. The other two phosphors were prepared too late in the program for evaluation, but are considered to be promising by analogy. The preparation of these phosphors is as follows:

4.4.1.2.1 Cadmium Sulfide (Ag,V) [Sample V-4]

A quantity of 7.3 grams of CdS, 1 ml of 0.01 M $AgNO_3$ (10^{-2} mmole), 1 ml of 0.01 M NH_4VO_3 (10^{-2}mmole) and 6 ml of water were mixed to form a paste. After drying for three hours at 120°C, the product was ground in a mortar and pestle and 3.5 ml of water added. The mass was mixed well and refired at 950°C for three hours in an H_2S atmosphere. After cooling to room temperature the product was reground and then refired for 1.5 hours at 950°C.

4.4.1.2.2 Cadmium Sulfide (Cu,V) [Sample V-3]

A quantity of 14.5 grams of CdS (0.1 mole), 2 ml of 0.01 M NH_4VO_3 (2×10^{-2} mmole V), 2 ml of 0.01 M $Cu(NO_3)_2$ (2×10^{-2} mmole Cu) and 7 cc of water were mixed and dried at 120°C for three hours. The material was then ground to a fine powder in a mortar and pestle. A quantity of 0.3 cc of 1 M $Cu(NO_3)_2$, 0.3 cc of 0.01 M NH_4VO_3 and 5 cc H_2O were mixed with the dry CdS and the mixture was dried at 120°C. The dry phosphor was then fired in an H_2S atmosphere at 950°C for one hour. The product was cooled to room temperature, ground to a fine powder and refired at 950°C for two hours.

4.4.1.2.3 Zinc Sulfide (Cu,V) [Sample V-5b]

A quantity of 9.7 grams (0.1 mole) of ZnS, 2 ml of 0.01 M NH_4VO_3 (2×10^{-2} mmole V) and 2 ml of 0.01 M $Cu(NO_3)_2$ (2×10^{-2} mmole Cu) were mixed to form a slurry, which was then dried at 120° for three hours. The product was ground in a mortar and pestle and 3.5 ml of water were added to give a thick paste. After drying at 120°C the powder was fired in an H_2S atmosphere at 950°C for one hour. After cooling to room temperature the product was reground to a powder and then refired at 1100° for one hour.

4.4.1.2.4 Cadmium Selenide

A series of CdSe phosphors were prepared to determine the effect of preparative technique on the emission. General Electric Company electronic grade CdSe 118-6-4 was uniformly mixed as an aqueous slurry with Fisher Certified $Cu(C_2H_3O_2)_2.H_2O$ and Fairmount Chemical Com $In(NO_3)_3$. The aqueous slurry was oven dried at 125°C. Cu and In were present as 0.02 mole percent and as 0.09 mole percent.

In the simpler preparation, the oven dried CdSe was packed into a quartz crucible, covered and placed in a larger quartz crucible filled with fired ZnS and covered. This was fired in a muffle furnace at 1000°C for one hour and then air cooled.

The CdSe was also fired in an atmosphere of H_2Se and H_2 for one hour at 1000°C. The CdSe was packed into a small quartz tube sealed at one end. This tube was inserted into the far end of a tapered quartz combustion tube which extended through two Hevi-Duty Electric Co. furnaces. A quartz boat with ASARCO Se, 99.999% pure Se was stationed at the near end. The combustion train was purged with Matheson ultrapure Hydrogen at room temperature and then inserted into the furnaces under H_2 flow with its CdSe and Se portions maintained at 1000°C and 500°C, respectively, for one hour. The tube was cooled to room temperature in its atmosphere of hydrogen, and then opened to the atmosphere.

In another group of phosphors, 50% of the CdSe was substituted by an equal amount of RCA electronic grade CdS 33-C-291A. The formulations were doped, dried, and fired under the conditions outlined for the CdSe phosphors.

4.4.2 Phosphor Test and Evaluation

The phosphors have three characteristics of particular interest: the exciting spectrum, the emitted spectrum, and the radiant efficiency. The important absorption peaks of the phosphor should match well the emission wavelengths of the laser excitation source. The latter in the case of ruby is well known - 6943A with a bandwidth of less than 1A. The emission spectrum of the phosphors were measured whenever possible. The phosphor efficiency, perhaps the most important of the three, was measured carefully and accurately.

4.4.2.1 Sample Preparation

The sample phosphors were mounted on index cards. The cards were first coated with adhesive by using double backed adhesive tape. The phosphor samples were ground to a powder and then sprinkled on the adhesive. In this manner, the phosphor was spread on a flat surface in a fairly uniform manner. The adhesive in no way covered the sample, thus providing a direct measurement of the phosphor efficiency. No binding agents were used that might interfere with the basic phosphor measurements.

4.4.2.2 Ultraviolet Excitation

Ultraviolet (UV) illumination was provided by a xenon flash tube which produced an arc 1/4" in length and 1 mm in width. The exit hole in the lamp cover was covered by a pair of glass color filters with a peak transmission at 360 millimicrons as shown in Figure 22. This filter was chosen because its peak transmission is very close to the wavelength (347 millimicrons) corresponding to a frequency doubled output of a ruby laser, a proposed source for stimulating UV phosphors.

The flash tube was calibrated by means of a direct comparison technique. A photodiode was illuminated by the calibrated incandescent lamp previously used to calibrate the photometer. The output for the known input was recorded thereby calibrating the diode. The calibrated lamp was then replaced by the filtered flash tube and the detector output was again recorded. Since the photodiode exhibits linear sensitivity over the intensity range observed, the flash tube brightness was determined.

UNCLASSIFIED

UNCLASSIFIED

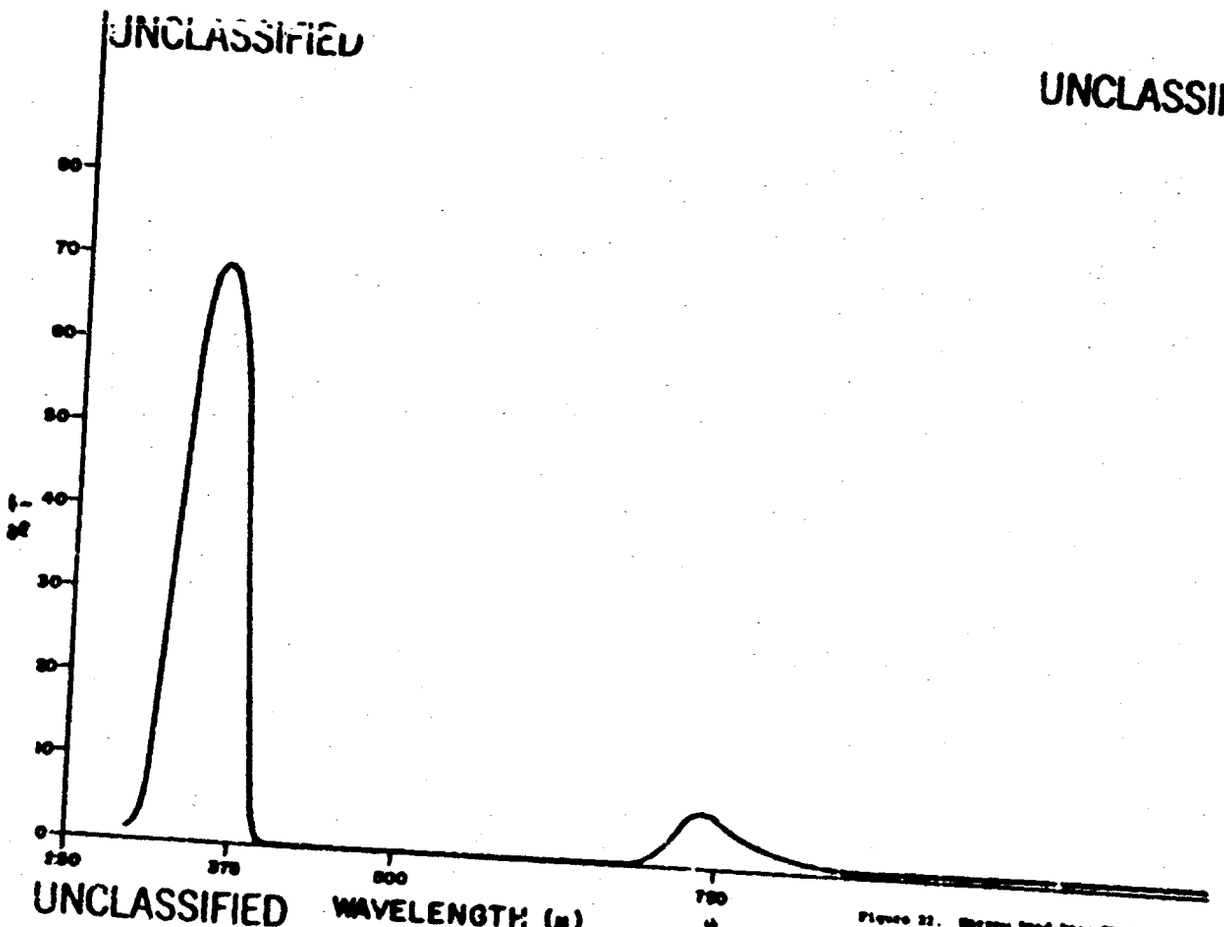

UNCLASSIFIED

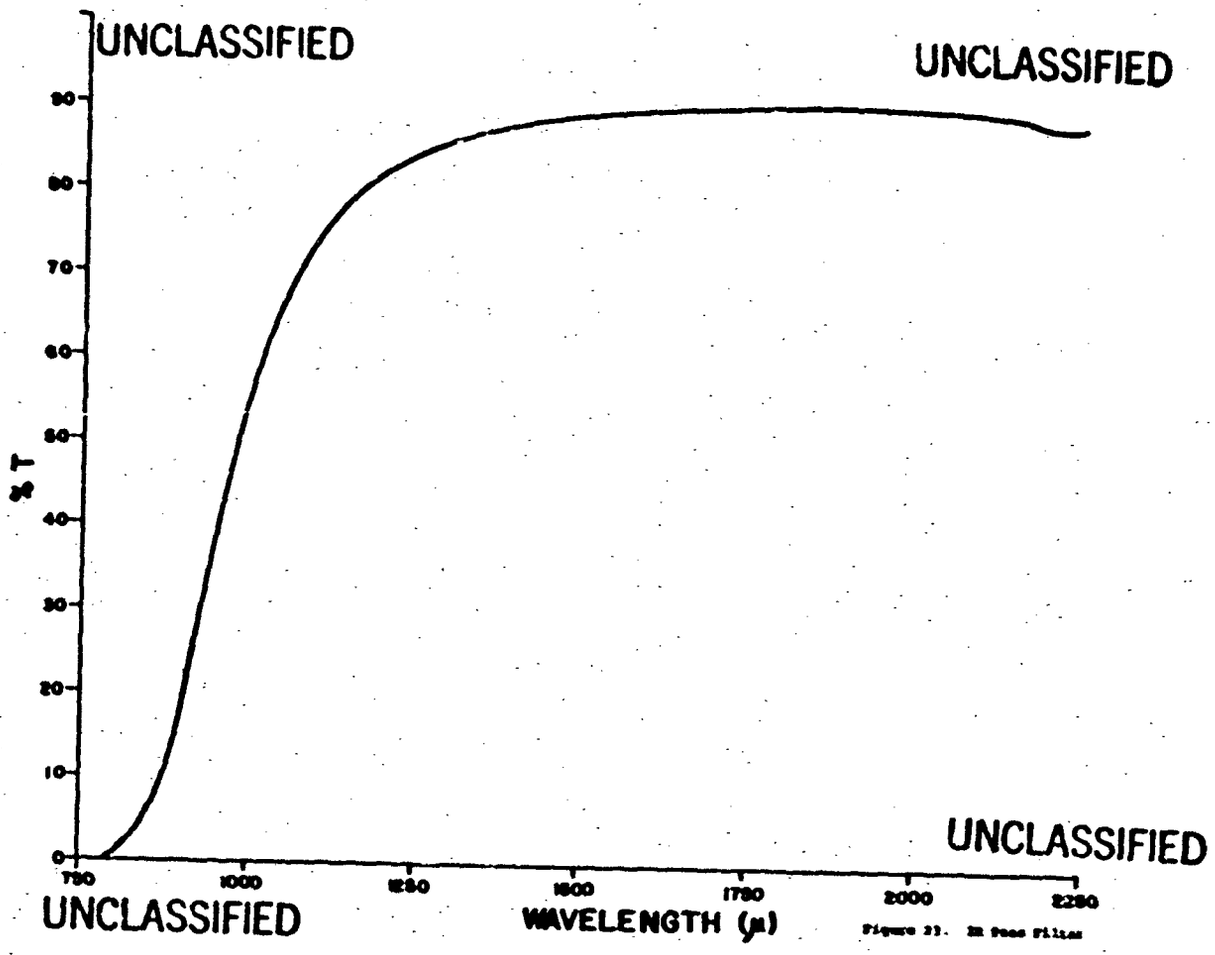

Figure 23. IR Band Filter

UNCLASSIFIED

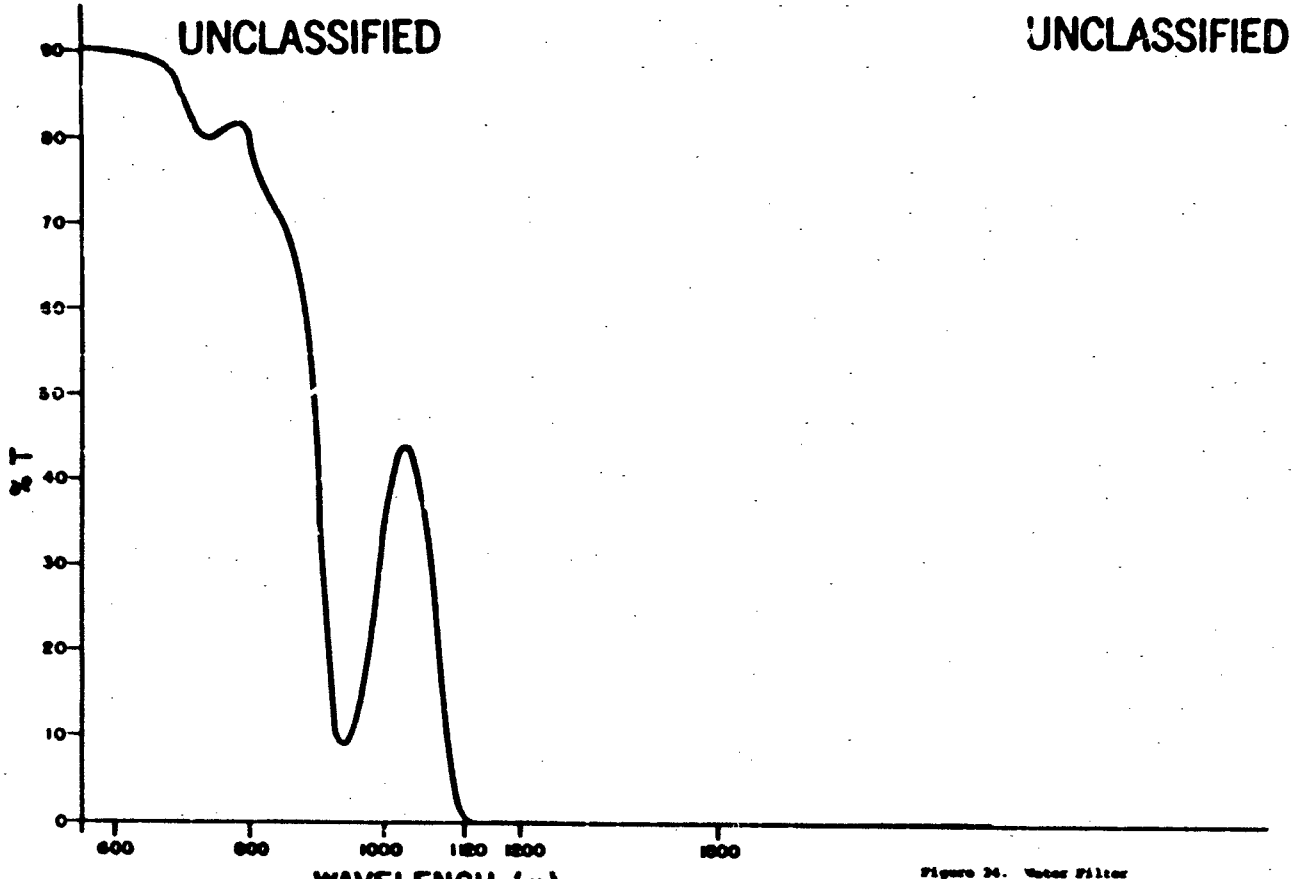

UNCLASSIFIED

UNCLASSIFIED

Figure 24. Water Filter

UNCLASSIFIED

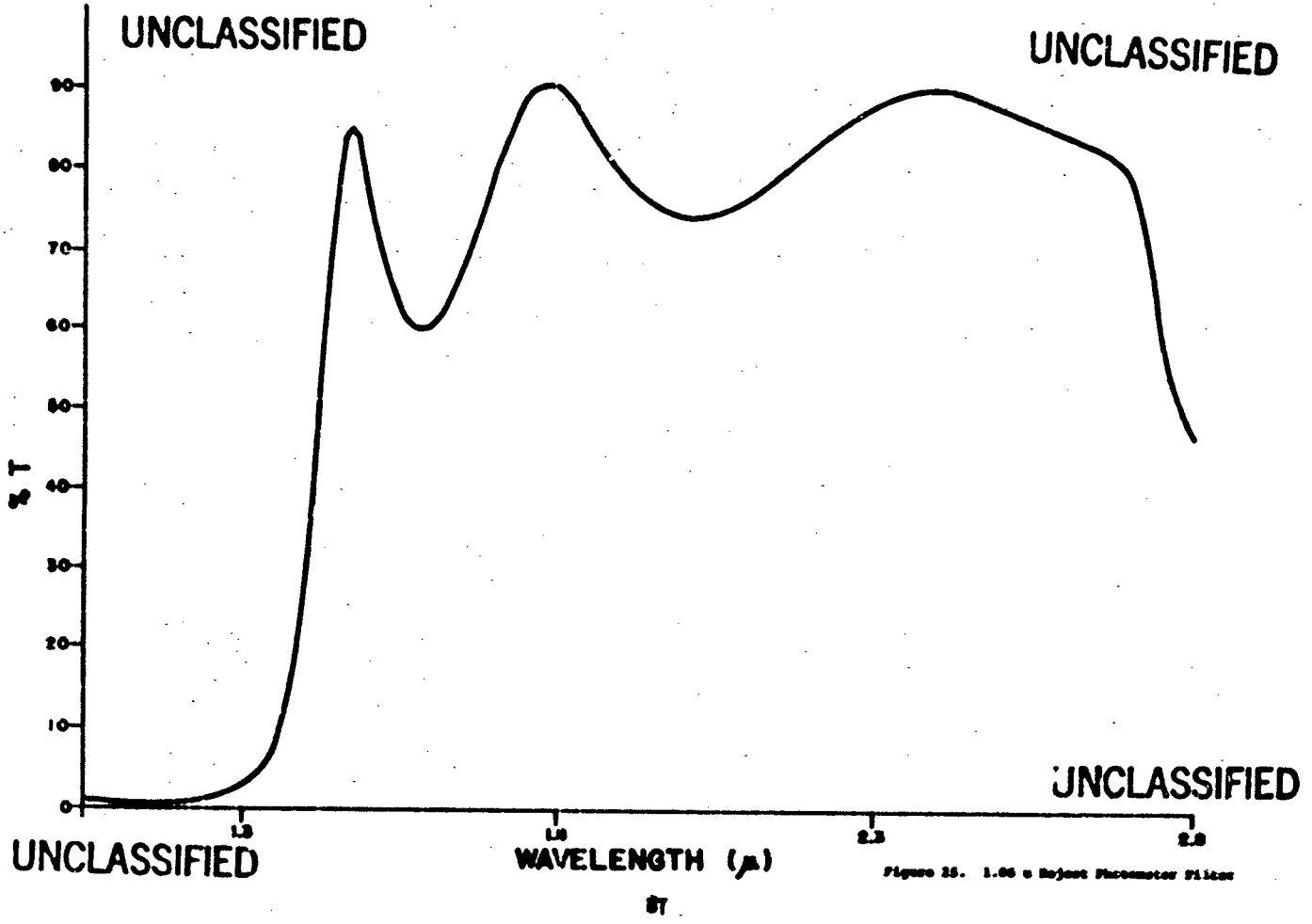

Figure 25. 1.06 u Reject Monochrator Filter

ST

4.4.2.3 Ultraviolet Phosphor Measurements

The ultraviolet phosphor measurements were made by illuminating the samples with the calibrated source and detecting the return signal with the calibrated photometer. The photometer aperture was masked with a pair of color glass filters exhibiting the transmission characteristics shown in Figure 23. These filters restricted the efficiency measurement to the infrared (IR) region of the spectrum and filtered out most of the exciting light, allowing the re-emission to be measured directly rather than as part of a sum of the bright illuminating source and the naturally weaker phosphor emission.

The phosphor sample cards were assumed to radiate as perfect diffuse radiators. The range equations, derived in Section 3 of this report, were adapted for the short distances involved in these test measurements. These equations were used to calculate the detector output assuming a 100% phosphor efficiency. The ratio of the measured to the calculated detector voltages was defined as the phosphor efficiency.

4.4.2.4 Infrared Excitation Source

The infrared phosphor excitation was supplied by an incandescent lamp, mounted in a parabolic reflector with an accompanying filter system. The filter consisted of a 5 cm thick water filter and a colored glass filter. The transmission characteristics of the filters are shown in Figures 23 and 24. By using combinations with various cutoff color filters it was possible to roughly determine the wavelength region of maximum excitation efficiency.

The IR excitation source was not calibrated since the photometer could be and was used directly, to compare the excitation to the emission of the phosphor.

4.4.2.5 Infrared Phosphor Measurements

The geometry of the IR phosphor measurements was similar to that for the UV phosphors. The phosphor efficiency was defined as the ratio of the watts per square centimeter of brightness from an emitting phosphor to that from a lossless diffuse surface. The former radiated a spectrum somewhere between 1 and 2.5 microns,

while the latter had the same spectrum as the lamp. A white index card served as the diffuse surface.

The photometer was masked by a filter system capable of transmitting all the re-emitted wavelengths but rejecting all the lamp output spectrum. With this filter in place, the phosphor emission was measured by the photometer. The filters were then removed and the phosphor replaced by an index card. The photometer output for the exciting and emitting spectrums, in combination with knowledge of the filter characteristics led to a direct measurement of the phosphor efficiency. The photometer filters consisted of a silicon window and interference filters, the combination exhibiting the transmission characteristics shown in Figure 25.

4.4.2.6 Phosphor Emission Spectra

It is necessary that the emission spectrum of the phosphor lie within a useable window in the atmosphere. If, in addition, the emission bandwidth is narrow, then the signal-to-noise can be improved. The emission characteristics of promising phosphors prepared by the Phosphor Group were determined using the fluorescence attachment for the Beckman DK-2A spectrophotometer. The data obtained served not only to determine the usefulness of the phosphor, but provided information for guiding the phosphor development work.

4.4.3 Characteristics of Selected Phosphors

Figure 26, 27, and 28 show the infrared fluorescence spectra of CdS(Ag,V), ZnS(Cu,V) and CdSe (Cu,In). The spectra are fairly narrow, which is helpful in distinguishing the return signal from background. Figure 29 shows the fluorescence spectra of CdSe(Cu, In) and CdSe-CdS(Cu,In), both for the same excitation source. It is seen that the CdSe-CdS phosphor is more efficient. Fluorescence data on the CdSe system is not yet available, so that it is difficult to fully assess the significance of these curves.

The characteristics of the most promising IR-IR phosphors are as follows:

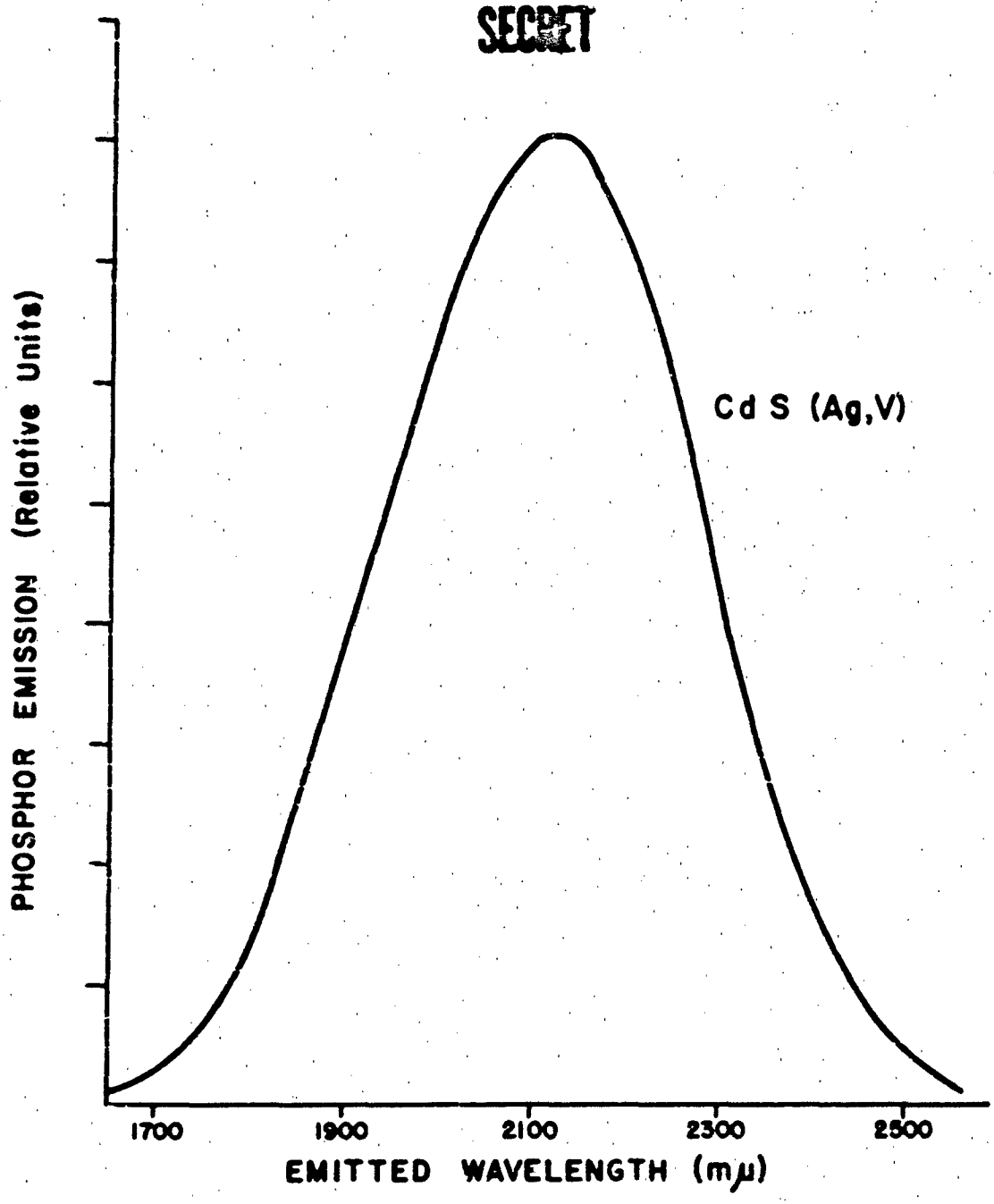

Figure 26 - Fluorescence Spectra of CdS(Ag,V)

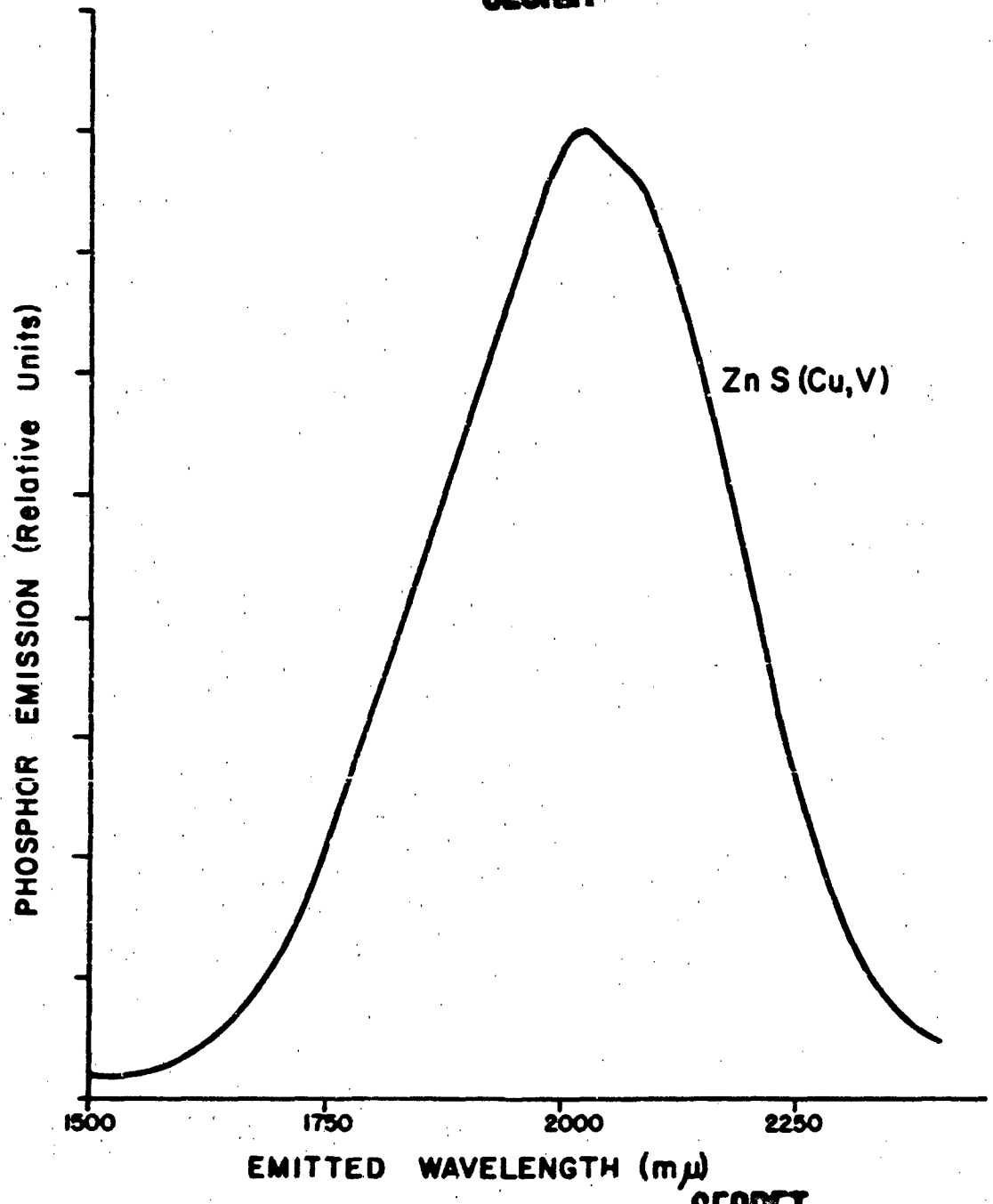

Figure 27 - Fluorescence Spectra of ZnS (Cu,V)

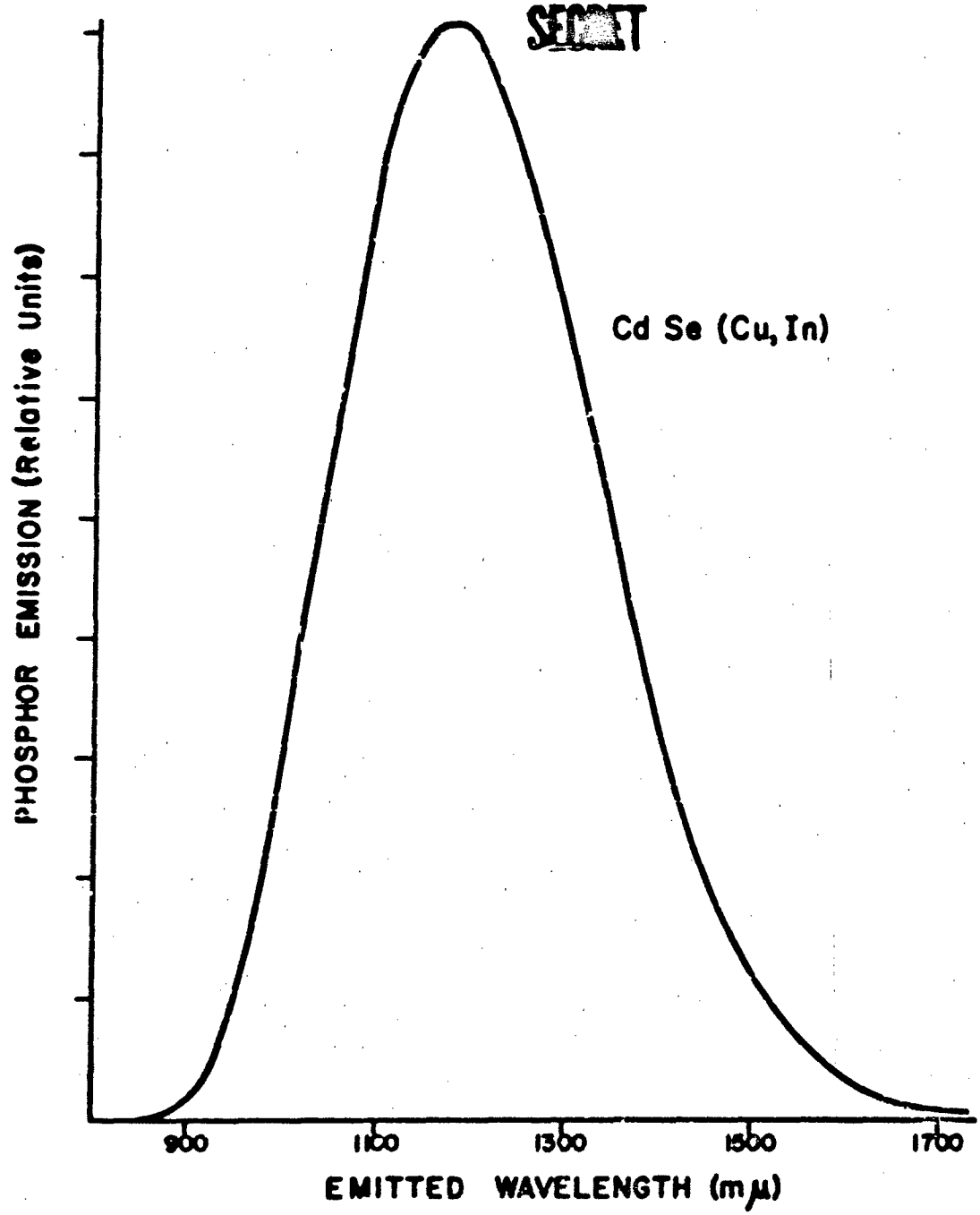

Figure 28 - Fluorescence Spectra of CdSe(Cu,In)

SECRET

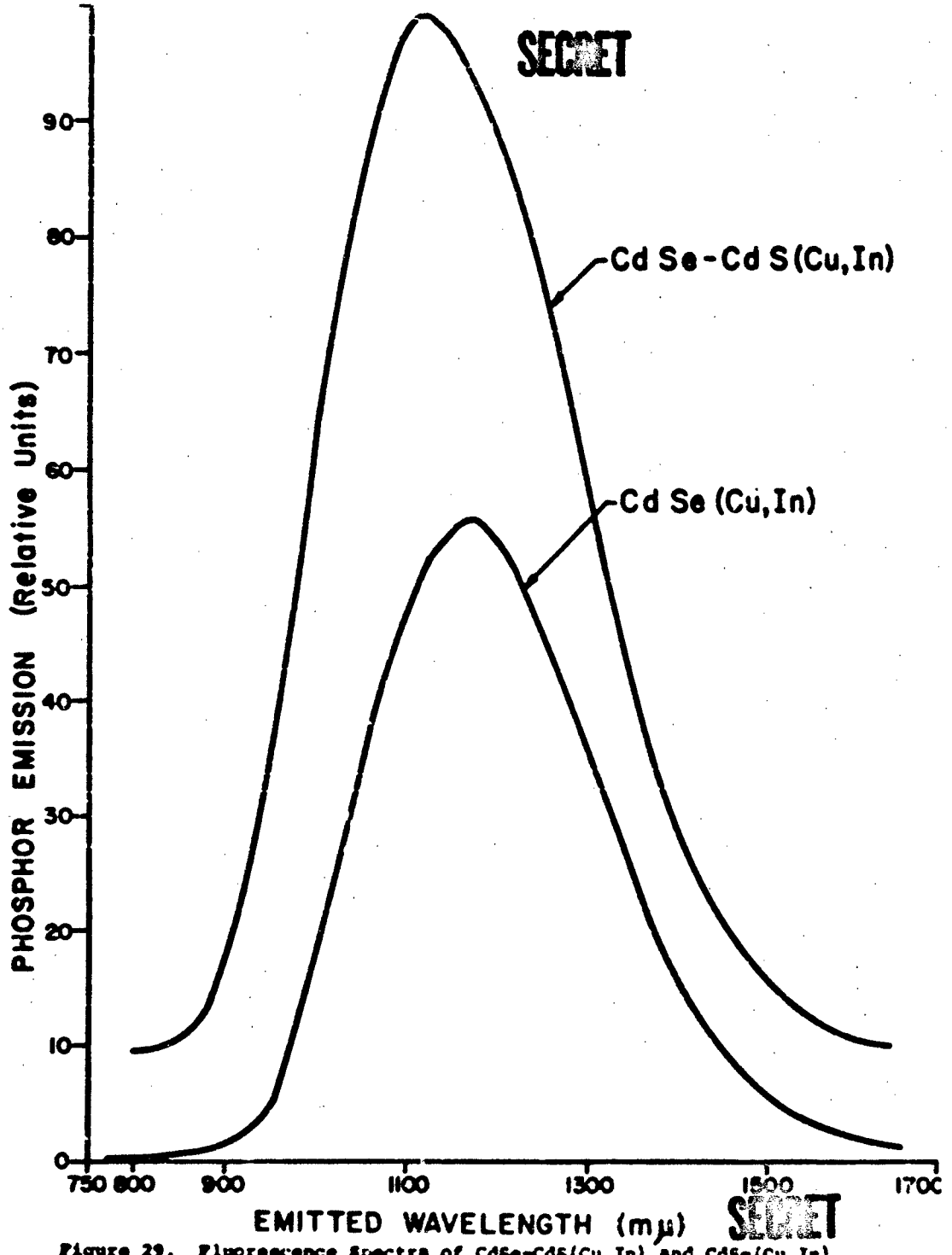

SECRET

Figure 29. Fluorescence Spectra of CdSe-CdS(Cu,In) and CdSe(Cu,In)

Formula	Excitation Wavelength Microns	Peak Emission Microns	Radiant Efficiency %
CdSe(Cu,In)	1.06	1.17	*
CdSe-CdS(Cu,In)	1.06	1.12	*
CdS(Ag,V)	1.06	2.13	*
ZnS(Cu,V)	1.06	2.03	4.0
CdS(Cu,V)	1.06	2.0	5.0

*Not yet measured

4.4.4 Toxicity of Phosphors

No tests were made to determine whether any of the phosphors had toxic properties. It is probable that ZnS will prove to be harmless; CdS may be a problem. Animal tests will have to be performed to determine the actual toxic hazard of promising phosphors.

4.4.5 Phosphor Dissemination Studies

A relatively small effort was made on the phosphor dissemination problem. Since the types or compositions of suitable phosphors were not known, it was only possible to make an exploratory study. Both inorganic and organic phosphors were considered.

The problem of disseminating an organic phosphor is considerably easier, since the phosphor can be dissolved in a suitable solvent. A resin or adhesive material can be added to the solution to aid in the fixation of the phosphor to the individual. Dissemination of the liquid can be carried out by available disseminators such as the USAF AN45Y-3 or the Army Interim Defoliant System.

A series of experiments were carried out in which a 1% solution of an organic phosphor was made in various resin solutions. Polyvinylpyrrolidone homopolymers and copolymers of ethyl acrylate, styrene and vinyl acetate were obtained from the General Aniline and Film Corp. The co-monomer presence tended to modify the aqueous solubility, flexibility and tackiness of the film. The PVP resins are available as emulsions, alcoholic and aqueous solutions and solids. All PVP resins that were formulated yielded good films. They included Polectron 130, Polectron 430, Polectron 825, K-15 PVP, K-30 PVP and I-335.

A typical formulation consisted of:

0.5 g. Blanchophor SV solution
2.0 ml Polectron 130 (copolymer emulsion)
250 ml H_2O
250 ml Isopropanol

Blanchophor is a ultraviolet excited phosphor emitting in the blue. Although not suitable as a marking agent, it served as a convenient organic test phosphor. The above formulation, when applied to skin, produced a thin film which exhibited strong fluorescence.

Formulations containing an insoluble inorganic phosphor separated out rapidly on standing. However, ballmilling restored the dispersion which yielded fluorescent films when used before settling occurred.

The Acryloid resins are polymers of the esters of acrylic and methacrylic acids and can be obtained as solids, or dissolved in organic solvents by the Rohm and Haas Co. The Rhoplex resins, also made by Rohm and Haas, are aqueous emulsions of acrylic polymers with functional groups. These polymeric resins are resistant to water and alcohol solvents and produce harder and tougher films than the polyvinylpyrrolidone group. Acryloid B-82 and Rhoplex AC-33 were formulated with 1% phosphor and aqueous isopropanol solvents to give films. On standing the phosphor settled out rapidly.

Acrylic emulsions CL-300 and CL-304 and a copolymer Vinyl Acrylic emulsion CL-222 were obtained from the Celanese Corp. Formulations were prepared with these emulsions to give films. It was found that settling of the inorganic phosphor in the following formulation occured slowly over several hours.

1.0 grams Sylvania 145
15.0 grams CL-304
75.0 ml Isopropanol

The Shawinigan Resins Corp. furnished Gelva Polyvinylacetate homopolymers and copolymers as a solid, solution or emulsion. The films obtained were not as hard, tough or water resistant as the acrylic films. Formulations were prepared from Gelva V-7 homopolymer and Gelva C-3V-10 and C-5V-10 copolymer resins.

The preparation of a stable, non-settling liquid dispersion of ZnS, CdS or similar inorganic phosphors will require a development study. It may be more desirable to dispurse these phosphors from a solid type disseminator. Both approaches should be considered.

4.1.6 Laser Excitation of Phosphors

A $CaWO_4$ (Nd^{3+}) laser was used to excite a phosphor sample card. The phosphor chosen was ZnS(Cu,V). The return signal from the phosphor was detected by the photometer and the output displayed on a Tektronix 555 dual beam oscilloscope. The results are shown in Figure 30. An analysis of the data shows that the return signal was of the order of magnitude predicted by the previous photometer experiments with a filtered xenon flash tube serving as a simulated laser source of 1.06 micron radiation.

UPPER TRACE: Laser Irradiating Signal (1.06 Microns)
LOWER TRACE: Return Signal From Inactive White Panel

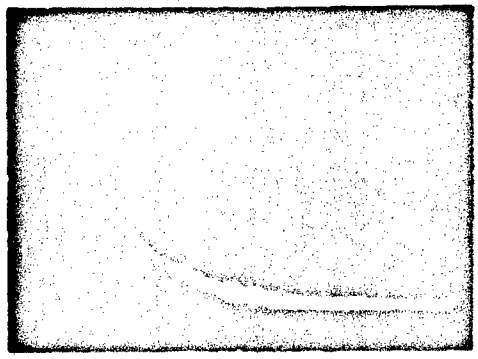

UPPER TRACE: Laser Irradiating Signal (1.06 Microns)
LOWER TRACE: Return Signal From White Panel Coated With Infrared Phosphor

Figure 30. $CaWO_4$ (Nd^{3+}) Excitation of a Phosphor

5. SUMMARY AND CONCLUSIONS

The analysis and experimental data show that the Isomet marking and detection system is feasible. A brief summary of the salient results and accomplishments follows:

5.1 System Components

The sector point marking system is composed of a phosphor, a phosphor disseminator, an optical transmitter and an optical receiver.

5.1.1 Phosphors

Three infrared emitting phosphors with characteristics suitable for use as a marking agent were developed during the study; Cd S (Cu), Zn S (Cu, V) and Cd S (Cu, V). These samples exhibited radiant efficiencies of two, four and five percent, respectively.

The excitation of a Zn S (Cu,V) phosphor panel by a $CaWO_4$ (Nd^{3+}) laser, and the detection of the infrared emission from the phosphor was successfully demonstrated in the laboratory and confirms the analytical analysis.

5.1.2 Dissemination of Phosphors

An exploratory study was made of the problems of disseminating phosphors suitable for use as marking agents. Considerable further work is needed to develop stable, non-settling liquid dispersions of inorganic phosphors such as ZnS or CdS, that could be disseminated with disseminators already developed. It may be more desirable to disseminate these phosphors in dry form.

5.1.3 Optical Transmitter

The only known means for achieving a beam of sufficiently high intensity with suitable collimation is a laser. The various laser characteristics such as pulse repetition rate, optical pumping, laser peak power, optical damage, optical cavity, cooling requirement, and type of laser material were intensively studied. A laboratory laser was built to help verify and optimize design concepts.

A $CaWO_4$ (Nd^{3+}) or neodymium glass laser has been shown to be a suitable radiation source for the airborne weapons system under study. Units capable of producing one-half to one megawatt pulses at pulse repetition rates up to fifty pulse per second can be reliably achieved.

An optical transmitter for close on-ground covert inspection of personnel could utilize either a laser or a filtered flash lamp.

5.1.4 Optical Receiver

A suitable receiver would have a catadioptric optical system with a clear aperture of from six to ten inches depending upon the application. The detector would be a photo conductive cell with a detectivity D* of up to 10^{12} cm $(cps)^{+1/2}$/watt.

5.2 System Characteristics

The characteristics of the system were analyzed in Section 3. By combining the equations from the system analysis with the experimental results, the characteristics of a feasible state-of-the-art weapons system for marking and detection can be evaluated. A projection is also made of the system performance that can be expected in the next five years by a reasonable extrapolation of the characteristics of the critical system components.

The system parameters are given below with the calculated system characteristics:

K_1 = 5% efficient	A_p = 200 cm^2
P.P = 0.5 megawatts	D^* = 10^{12} cm$(cps)^{1/2}$/watt
t = 0.02 sec	S/N = 5
ϕ = 0.2 radian approx. 12°	f# = 1
θ = 0.1 radian approx. 6°	T = 10^{-6} sec
D_o = 25 cm	V = 300 knots

R_{max} = 1300 feet
$(V/R)_{max}$ = 5 sec^{-1}
R_{min} = 20 feet

These are typical numbers and show that the system is operable from the deck to 1300 feet. The (V/R) limitation means that the system is limited to 300 knots at 100 feet; 600 knots at 200 feet,

[redacted]

[redacted]

and so linearly up to 3600 knots at 1200 feet. The path width is 20 feet at 100 feet and increases linearly with altitude to 260 feet at 1300 feet. It should be noted that the system works well at any velocity below those stated, at lower altitudes the signal to noise ratio is higher. For a 300 knot aircraft, the system is operable anywhere from 100 feet to 1300 feet.

An outstanding feature of the system is the capability that it gives a high performance aircraft, such as an F-104, to examine a 200 foot wide swath of terrain at top speed from 1000 feet. This aircraft could also, with the same system and no adjustments, slow down to 300 knots and check out a 20 foot swath from 100 feet up.

The projected system parameters are

K_1 = 50% efficient	A_p = 200 cm^2
P.P = 50 megawatts	D^* = 10^{13}
t = .005 sec.	S/N = 5
ϕ = 0.2 rad approx. 12°	$f\Phi$ = .1
θ = 0.005 rad approx. .29°	T = 10^{-7} sec
λ = 25 cm	V = mach 1

R_{max} = 32,400 feet
$(V/R)_{max}$ = 11 (sec^{-1})
W_{min} = 20 feet

The (V/R) value is twice what it was previously. This means the vehicle could operate at Mach 1 at 100 feet while examining a 20 foot swath. The unit will remain in operation up to 18,000 foot altitudes. This system should satisfy most mission requirements.

The values used for θ and ϕ can be changed to suit the particular application. Increasing θ and ϕ increases the value of the (V/R) ratio and the path width, respectively. At the same time these increases lower the system ceiling. The values chosen as typical values should not be considered to be limits.

[redacted]

[redacted]

[redacted]

6. RECOMMENDATIONS

The [redacted] of the Isomet sector-point airborne marking and detection system is considered highly promising, and warrants a substantial advanced development program. Table 11 indicates the logical sequence of phases and time scheduling required to lead to a final weapons system. Phase 1 refers to the feasibility study described in this report.

It is recommended that the next effort consist of two concurrent phases. Phase 2 comprises the design and construction of a prototype to demonstrate the feasibility of the system using an operational aircraft. Phase 3 is a continuing research and development effort designed to optimize the subsystems and to improve the overall system capabilities. Phase 3 would insure that the state-of-the-art would be advanced while the prototype is being built.

6.1 General Features of Prototype

In order to demonstrate the feasibility of the system it is proposed that a flyable prototype be built embodying the concepts described above. This prototype will be capable of detecting marked objects or personnel in a search swath on the ground from an aircraft moving at velocities up to 300 knots. This swath will be approximately 80 feet wide at a 200 foot aircraft altitude.

6.2 Detailed Characteristics of Prototype

The airborne prototype will consist of three basic units: the transmitter, the receiver and the cine camera. These elements are shown in the block diagram in Figure 31.

The transmitter will be a Q-switched laser with a field of view of $5^{\circ} \times 20^{\circ}$. Its output characteristics will be adequate to provide a detectable return from phosphors having an equivalent area of 200 cm^2.

The receiver, which detects the radiation emitted from the phosphor, will consist of an optical system which will focus the invisible radiation from the phosphor onto a photoconductive detector. The receiver sensitivity will be essentially limited by the state-of-the-art capabilities today.

[redacted]

[redacted]

[redacted]

SYSTEM DEVELOPMENT SCHEDULE

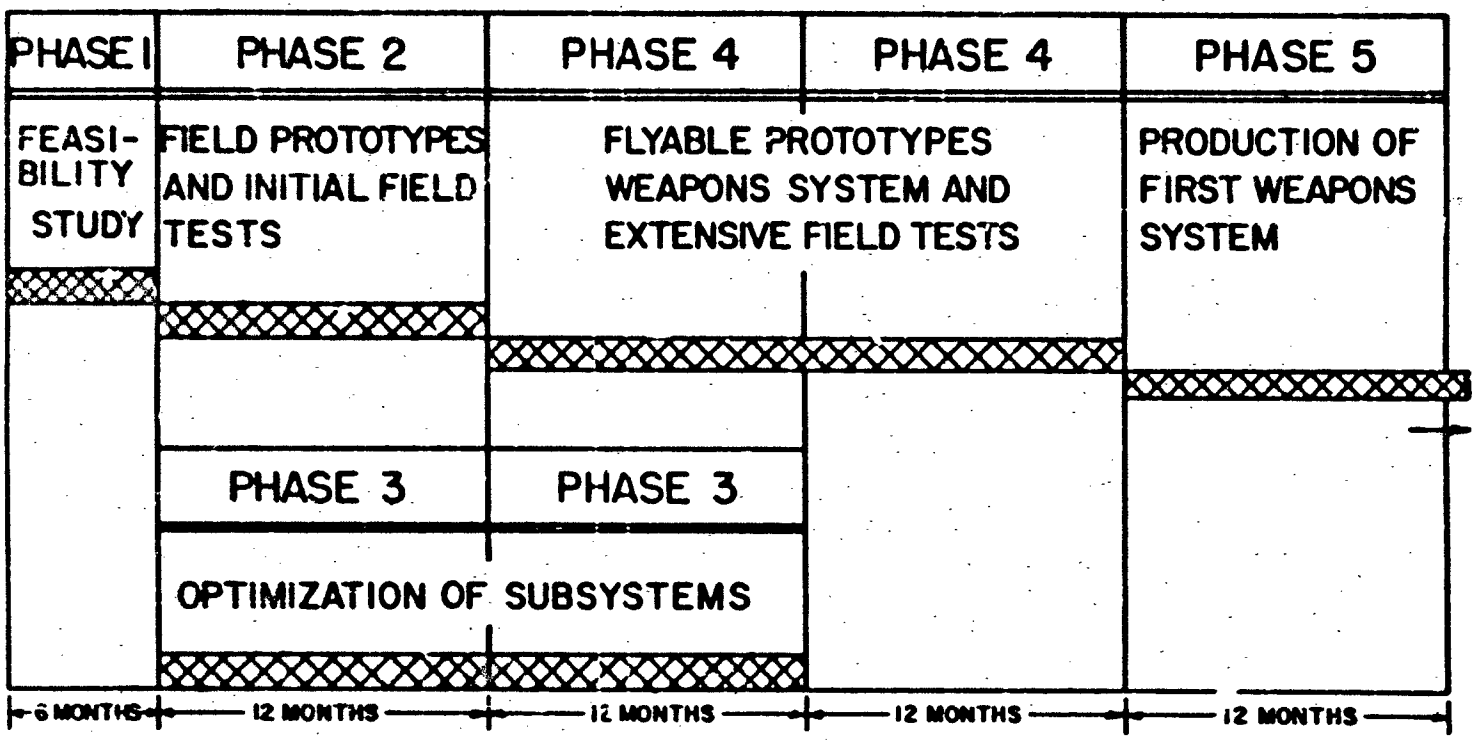

TABLE 11

[redacted]

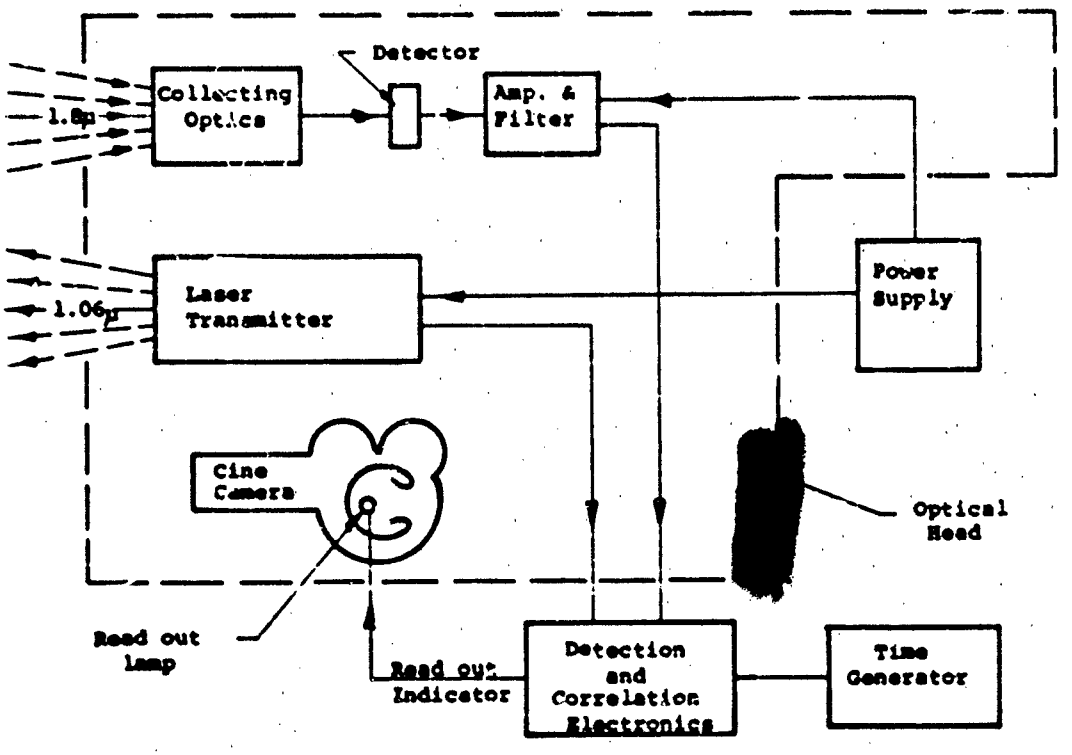

Figure 31 System block diagram

Read-out for the prototype will be provided by a 16 mm cine camera boresited to the transmitter. This camera will provide a pictorial record of the terrain under surveillance. It will serve to correlate detected marked objects with the terrain being photographed. Located in the cine camera will be a small neon bulb which will be flashed each time a return is detected by the receiver. This flash will illuminate a portion of the films thus identifying the frames which contain marked objects.

Auxiliary equipment will consist of special power supplies and electronic equipment necessary for the operation of the prototype. This equipment will be packaged so as to utilize existing cargo tie-downs in the aircraft. Packaging will be such that minimum modification to an aircraft will be necessary for the installation of the prototype.

The input power requirement will be approximately 1 KVA. It is expected that such a power level will be available from the aircraft supply during flight, and from a gasoline-powered motor-generator set during ground check out and test.

6.3 Future Effort Beyond Phases 2 and 3

After the satisfactory demonstration in the field of the Decomat marking and detection system, the information gleaned from Phases 2 and 3 can then be utilized to design and build a high performance prototype for flight tests and evaluation of the entire system. Successful conclusion of Phase 4 would then lead the way to the production of operational weapon systems.

[redacted]-4

Security Classification

DOCUMENT CONTROL DATA · R&D

(Security classification of title, body of abstract and indexing annotation must be entered when the overall report is classified)

1 ORIGINATING ACTIVITY (Corporate author) Isomet Corporation Palisades Park, N. J.	2a REPORT SECURITY CLASSIFICATION SECRET 2b GROUP GP-4

3 REPORT TITLE PERSONNEL MARKING AND DETECTION (LASER TECHNIQUE)

4 DESCRIPTIVE NOTES (Type of report and inclusive dates)
Final Report

5 AUTHOR(S) (Last name, first name, initial)

6 REPORT DATE April 1965	7a TOTAL NO. OF PAGES 93	7b NO. OF REFS
8a CONTRACT OR GRANT NO. AF 08(635)-3784 b PROJECT NO. 6980 c d	9a ORIGINATOR'S REPORT NUMBER(S) ATL-TP-65-32 9b OTHER REPORT NO(S) (Any other numbers that may be assigned this report)	

10 AVAILABILITY/LIMITATION NOTICES
Qualified users may obtain copies of this report from the Defense Documentation Center

11 SUPPLEMENTARY NOTES	12 SPONSORING MILITARY ACTIVITY Det 4, Research and Technology Division Air Force Systems Command Eglin Air Force Base, Florida

13 ABSTRACT

(S) Calculations and experimental studies have been made of the Isomet system for marking and detection of individuals. Results of these studies indicate that the system is feasible. Recommendations are presented for the further development of this weapon system.

DD FORM 1473

[redacted]-4

Security Classification

[redacted]-4

Security Classification

KEY WORDS	LINK A		LINK B		LINK C	
	ROLE	WT	ROLE	WT	ROLE	WT
Marking personnel						
Detecting personnel						
Airborne delivery						
Phosphor agents						
Laser detection						
IR region						
UV region						

INSTRUCTIONS

1. **ORIGINATING ACTIVITY:** Enter the name and address of the contractor, subcontractor, grantee, Department of Defense activity or other organization *(corporate author)* issuing the report.

2a. **REPORT SECURITY CLASSIFICATION:** Enter the overall security classification of the report. Indicate whether "Restricted Data" is included. Marking is to be in accordance with appropriate security regulations.

2b. **GROUP:** Automatic downgrading is specified in DoD Directive 5200.10 and Armed Forces Industrial Manual. Enter the group number. Also, when applicable, show that optional markings have been used for Group 3 and Group 4 as authorized.

3. **REPORT TITLE:** Enter the complete report title in all capital letters. Titles in all cases should be unclassified. If a meaningful title cannot be selected without classification, show title classification in all capitals in parenthesis immediately following the title.

4. **DESCRIPTIVE NOTES:** If appropriate, enter the type of report, e.g., interim, progress, summary, annual, or final. Give the inclusive dates when a specific reporting period is covered.

5. **AUTHOR(S):** Enter the name(s) of author(s) as shown on or in the report. Enter last name, first name, middle initial. If military, show rank and branch of service. The name of the principal author is an absolute minimum requirement.

6. **REPORT DATE:** Enter the date of the report as day, month, year, or month, year. If more than one date appears on the report, use date of publication.

7a. **TOTAL NUMBER OF PAGES:** The total page count should follow normal pagination procedures, i.e., enter the number of pages containing information.

7b. **NUMBER OF REFERENCES:** Enter the total number of references cited in the report.

8a. **CONTRACT OR GRANT NUMBER:** If appropriate, enter the applicable number of the contract or grant under which the report was written.

8b, 8c, & 8d. **PROJECT NUMBER:** Enter the appropriate military department identification, such as project number, subproject number, system numbers, task number, etc.

9a. **ORIGINATOR'S REPORT NUMBER(S):** Enter the official report number by which the document will be identified and controlled by the originating activity. This number must be unique to this report.

9b. **OTHER REPORT NUMBER(S):** If the report has been assigned any other report numbers *(either by the originator or by the sponsor)*, also enter this number(s).

10. **AVAILABILITY/LIMITATION NOTICES:** Enter any limitations on further dissemination of the report, other than those imposed by security classification, using standard statements such as:

(1) "Qualified requesters may obtain copies of this report from DDC."

(2) "Foreign announcement and dissemination of this report by DDC is not authorized."

(3) "U. S. Government agencies may obtain copies of this report directly from DDC. Other qualified DDC users shall request through _____."

(4) "U. S. military agencies may obtain copies of this report directly from DDC. Other qualified users shall request through _____."

(5) "All distribution of this report is controlled. Qualified DDC users shall request through _____."

If the report has been furnished to the Office of Technical Services, Department of Commerce, for sale to the public, indicate this fact and enter the price, if known.

11. **SUPPLEMENTARY NOTES:** Use for additional explanatory notes.

12. **SPONSORING MILITARY ACTIVITY:** Enter the name of the departmental project office or laboratory sponsoring *(paying for)* the research and development. Include address.

13. **ABSTRACT:** Enter an abstract giving a brief and factual summary of the document indicative of the report, even though it may also appear elsewhere in the body of the technical report. If additional space is required, a continuation sheet shall be attached.

It is highly desirable that the abstract of classified reports be unclassified. Each paragraph of the abstract shall end with an indication of the military security classification of the information in the paragraph, represented as (TS), (S), (C), or (U).

There is no limitation on the length of the abstract. However, the suggested length is from 150 to 225 words.

14. **KEY WORDS:** Key words are technically meaningful terms or short phrases that characterize a report and may be used as index entries for cataloging the report. Key words must be selected so that no security classification is required. Identifiers, such as equipment model designation, trade name, military project code name, geographic location, may be used as key words but will be followed by an indication of technical context. The assignment of links, rules, and weights is optional

[redacted] GP-4

Security Classification

UNCLASSIFIED

UNCLASSIFIED